20

New Non-Destructive Methods of Diagnosing Health of Gas Turbine Blades

Józef Błachnio[1,2], Mariusz Bogdan[2] and Artur Kułaszka[1]
[1]*Air Force Institute of Technology, Warszawa,*
[2]*Technical University of Białystok, Białystok,*
Poland

1. Introduction

The illuminated blade/vane surface can be recognized by a light-sensitive detector (a CCD matrix with an optical system – an optoelectronic device) owing to the fact that the surface becomes a secondary source of light (Zhang et al., 2004; Rafałowski, 2004; Tracton, 2006, 2007). Therefore, it is possible to diagnose the examined object in an indirect way by the processing and analysis of information acquired as digital images (Bogdan; 2008; Błachnio & Bogdan, 2010). Only a very tiny portion of an incident light beam is absorbed by metallic surfaces. Most of the light (90-95%) is reemitted from the reflecting surface as visible light with the same wavelength as the incident light. The remaining 5-10% of the absorbed energy is dissipated as heat (according to the rule of energy conservation). Chemical composition of the coating matter that covers surfaces of metallic objects decides the attenuation of some wavelengths in the spectrum of illuminating light, whilst the mixture of light that is selectively reflected from a specific surface is decisive for the perception of colours (some metals may exhibit specific colours due to selective reflection of light, e.g. gold, copper) (Zhang et al., 2004; Tracton, 2006). The CCD matrix is a set of many light-sensitive sensors, where each sensor is capable to record and then reproduce an electric signal that is proportional to the amount of light that has illuminated the surface (the photoelectric effect – emission of electrons as a consequence of their absorption of energy from photons that reach the matter; the diagram of such energy conversion and the associated losses are shown in Fig. 1).
The image-recording devices usually incorporate colour filters that are installed just upstream the light sensors and enable the intensity of a particular bandwidth within the light spectrum (a certain bandwidth of visible electromagnetic waves) to be recorded at a given location of the matrix. After processing by the central unit (CPU) the acquired information can be stored as digital images (graphic files) (Rafałowski, 2004).
The analysis of histograms of digital images is very useful since it provides a great amount of information about the image that has been processed, including information about the range of brightness levels and the number of levels represented in the images. In the case of images acquired under suitable illumination conditions the histogram includes also quantitative information about the brightness of the image acquired for the photographed object. On the other hand, the 2-D co-occurrence matrices presented by Haralick in his studies (Haralick & Shanmugam, 1973; Haralick & Shapiro, 1992) are used for analyses of

textures as they are capable to extract spatial relationships from the image on the basis of the object brightness. Utilization of information acquired from histograms (statistical parameters such as: location of the maximum saturation, medians, quartiles, percentiles, average value, skewness, variance, kurtosis, the third and fourth central moments, excess) as well as that from co-occurrence matrices (such parameters as: energy, contrast, correlation, variance, homogeneity – the reverse differential moment, accumulated average, entropy) allows of the assignment of blade/vane surfaces to specific health levels. Based on the parameters found from histograms and from the co-occurrence matrices, with neural networks applied (the pattern recognition) it will be also possible to assign the blade image (recorded for a specific surface) to a defined class that corresponds with a given health level, i.e. the fit-for-use condition (Bogdan, 2009).

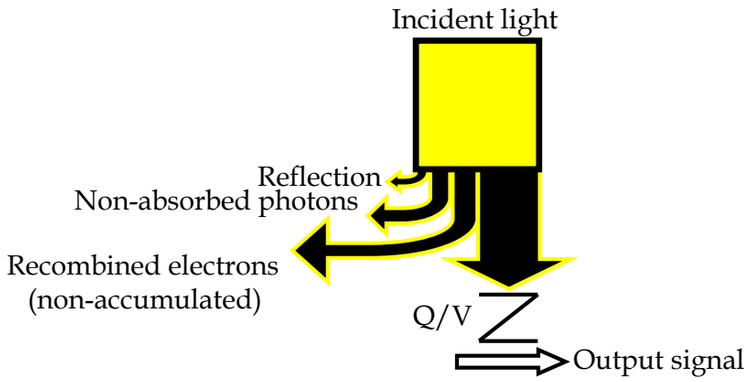

Fig. 1. Energy losses in the process of converting an optical signal into the electric one by means of a CCD cell (Rafałowski, 2004)

2. A method for the assessment of condition of new gas turbine blades (a laboratory experiment)

Subject to examination were new rotor blades of a gas turbine of aircraft jet engine. The blades are not cooled during the engine operation. They have been made from the nickel superalloy denoted as EI 867-WD (HN62MWKJu), suitable for the plastic working. This superalloy belongs to a sparse group of superalloys with no titanium admixture. The content of chromium is lower, therefore it is more susceptible to corrosion. For that reason various protective coatings are applied, e.g. aluminium ones. The TC 14-1-232-72 standard contains requirements for the chemical composition of the superalloy, thermal treatment and mechanical properties.

The research project assumed investigation of four new blades that were cut into four equal parts. To avoid structural alterations due to high temperature, the so-called 'grinding burns', the cutting was carried out with a wire electric erosion machine. Pieces of blades were randomly selected and soaked (three pieces at a time) in a vacuum furnace at five various temperature levels, with the increment of 100 K, starting with the temperature of 1023 K. Then the specimens were cooled down inside the furnace until the ambient temperature was reached. Values of temperature applied while soaking the blade specimens correspond to temperature ranges that occur under both regular and failure in-service modes of rotor blades operation. Temperature of the working-agent stream (exhaust gas) at

the outlet of the combustion chamber of the aircraft jet engine should remain in the range of 1173 K to 1223 K due to limitations imposed by thermal and chemical characteristics of materials used to manufacture solid and non-cooled blades of the gas turbine (Poznańska, 2000; Dżygadło et al., 1982; Kerrebrock, 1992; Hernas, 1999). Instances of short-term heating of blade material above the regular operating temperature quite often occur in the course of gas turbine operation. Therefore, such parameters as heat resistance and high-temperature creep resistance of the alloy to supercritical temperature are of crucial importance (Sieniawski, 1995; Sunden & Xie, 2010). The blades were cleaned in ultrasonic washers both before and after they were subjected to the soaking process.

The initial phase of metallographic investigation was focused on the determination of time the blade soaking process should take as it is the parameter that, along with the soaking temperature, affects the kinetics of growth and coagulation of the γ′ phase particles. For that purpose the experiment was carried out, which consisted in that the specimens were soaked at temperature of T_{4max} (the maximum temperature downstream of the turbine, i.e. 1223 K, over 0.5 h, 1 h, 2 h, and 3 h). Metallographic microsections of these specimens were prepared with conventional methods to be then etched with the reactant of the following chemical composition:

$$30\ \text{g}\ FeCl_2 + 1\ \text{g}\ CuCl_2 + 0.5\ \text{g}\ SnCl_2 + 100\ \text{ml}\ HCL + 500\ \text{ml}\ H_2O \quad (1)$$

Both an optical microscope and a scanning electron microscope (SEM) were used to observe the microstructure. This enabled acquisition of information on structural changes in both the coating and the parent material of the blades, the changes being dependent on the soaking time and mainly including modifications of the size and distribution of the γ′ phase (Fig. 2).

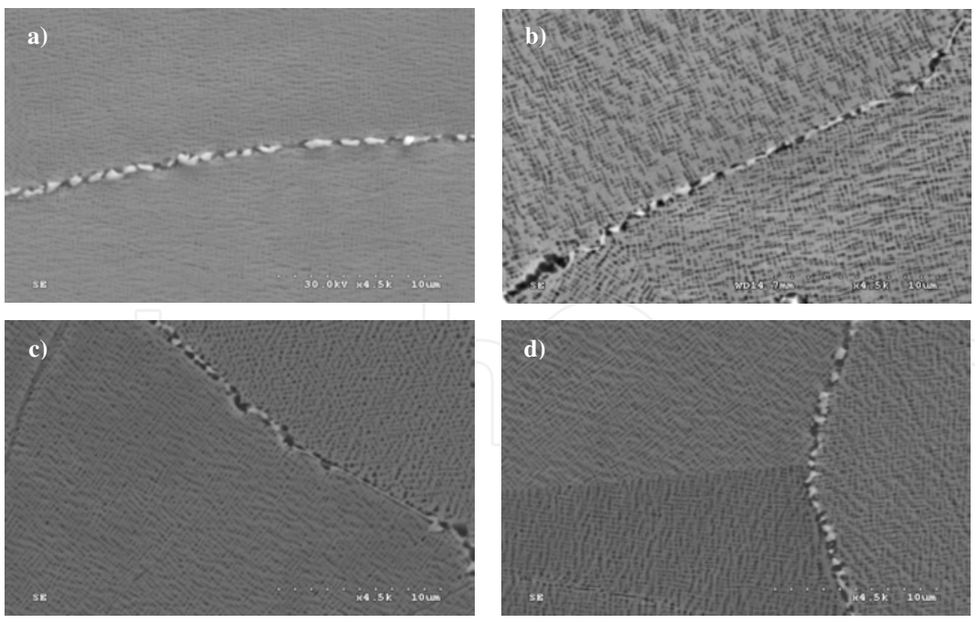

Fig. 2. Morphology of γ′ precipitates – soaking at temperature 1223 K over: a) 0.5 h, b) 1 h, c) 2 h, d) 3 h (magn. x4500)

The dedicated software to analyze images of the material microstructures (Bogdan, 2009) in was used to determine alterations in size (surface area) of precipitates of the strengthening γ′ phase against the soaking time (Fig. 3).

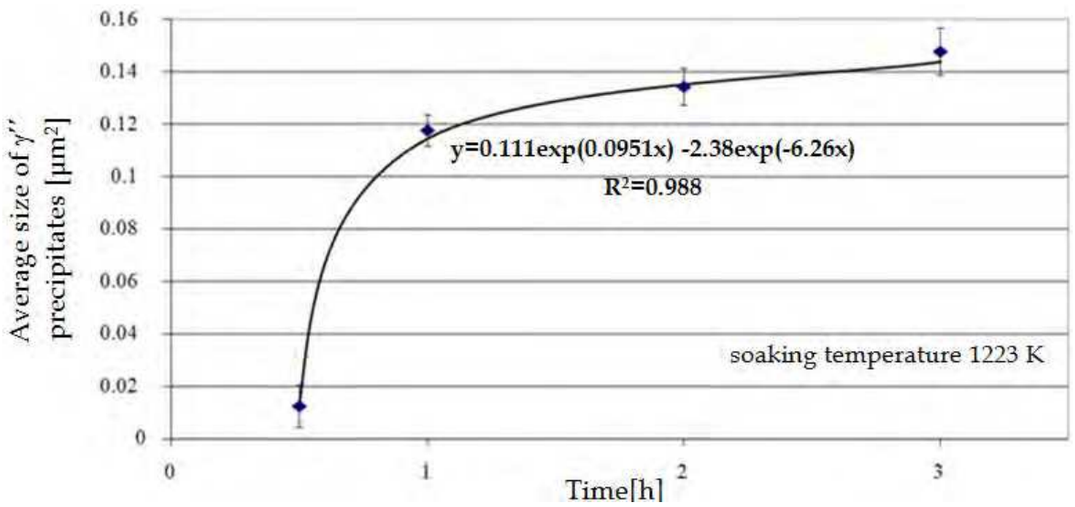

Fig. 3. Variations in the average size of γ′ precipitates against time of soaking the specimens

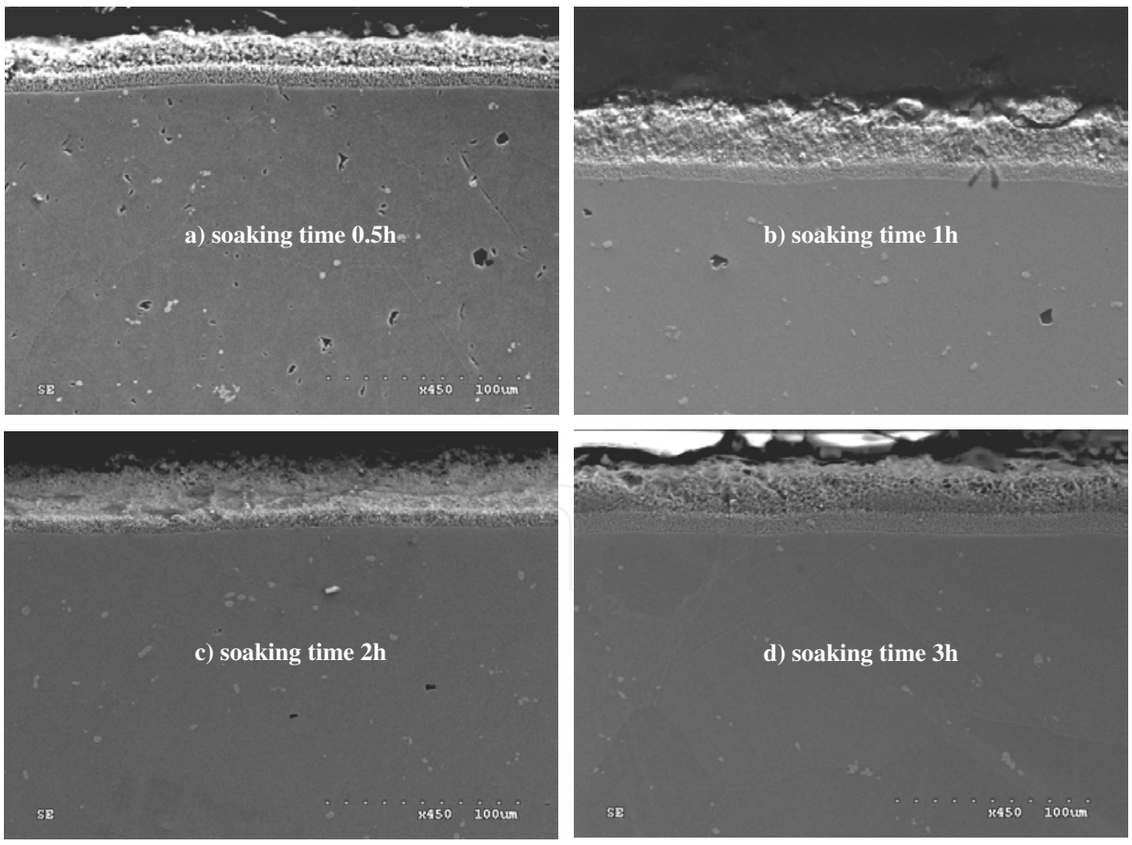

Fig. 4. Structure of the aluminium layer after soaking at temperature 1223 K over: a) 0.5 h, b) 1 h, c) 2 h, d) 3 h (magn. x4500)

The soaking time affected also the change in thickness of the aluminium protective coating (Fig. 4). The film thickness is calculated on the basis of ten distances measured in pixels (d_n, n = 1, 2, 3, … 10) – Fig. 5. The obtained distances (in pixels) were then multiplied by the scale parameter, i.e. the size of one pixel in μm. In that way the value of average thickness for the aluminium coating was calculated for each of the recorded (and then analyzed) images. The coating thickness was measured at three locations, i.e. on the leading edge, in the centre, and on the trailing edge of the blade. Fig. 6 presents averaged values of the protective coating thickness for various soaking times. On the basis of graphs in Fig. 3 and Fig. 6, for the needs of examining the effect of high temperatures onto the blade material, the soaking time was assumed to be 1h at constant temperature, i.e. 1223 K. It was the time when rapid growth in the size of particles of the γ′ phase occurred, with only slight increase in the coating thickness.

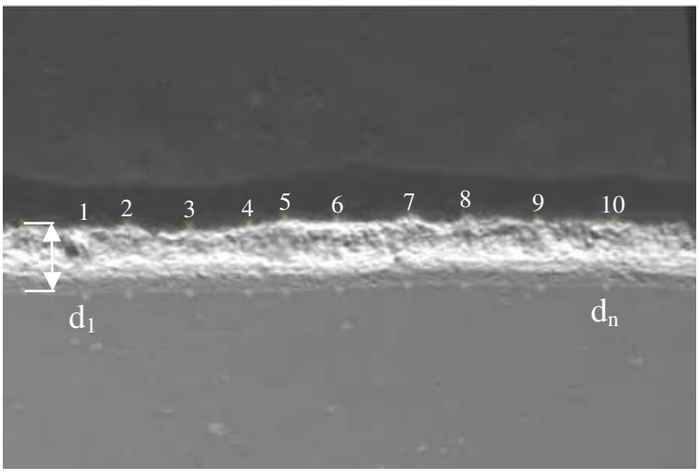

Fig. 5. Measurement of coating thickness

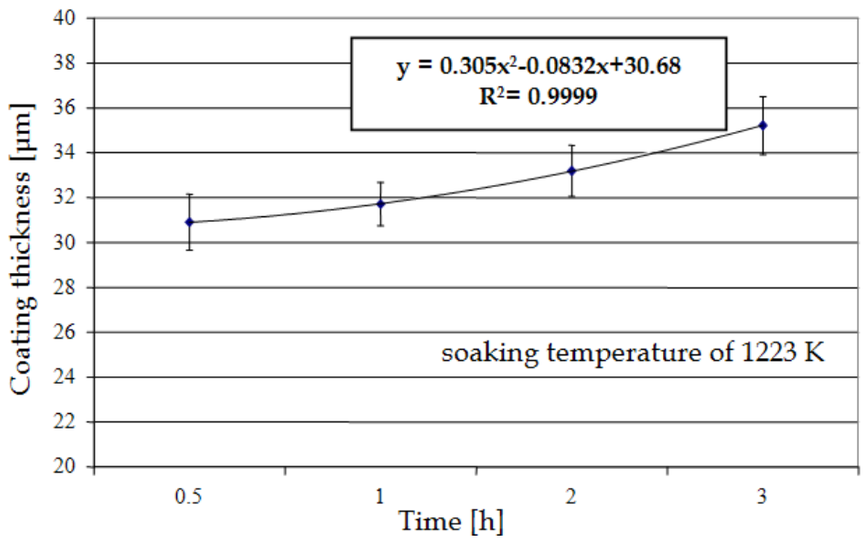

Fig. 6. Soaking–time dependent variation in thickness of the protective coating

Images of surfaces of blade specimens were acquired both before and after specimens soaking in the furnace. The photos were taken on a purpose-built workbench (Bogdan & Błachnio, 2007; Błachnio & Bogdan, 2008;) with a digital photo camera, while the surfaces were illuminated with scattered white light. Repeatability of the obtained results was proved by taking multiple photos of the same specimens, under the same conditions with appropriate settings of parameter of the digital photo camera. The soaking of blade specimens in the furnace led to alterations in colour of the surfaces. An exemplary set of images is shown in Fig. 7.

Fig. 7. Images of surfaces of specimens soaked at various temperatures

It was also determined how the temperature of blade soaking affects their microstructures. Examination was carried out using metallographic microsections and both an optical and a scanning electronic microscope (SEM). Fig. 8 shows the (new) blade structure before soaking. One can see the coating of the aluminium alloy (Fig. 8a) diffused in the blade parent metal as well as cuboidal precipitates of the γ′ phase of the alloy (Fig. 8b).

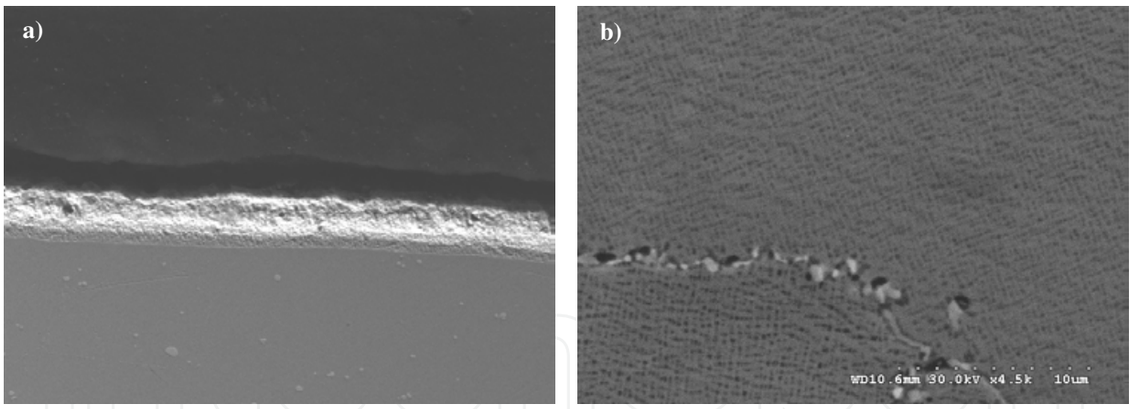

Fig. 8. Metallographic structure of the blade prior to soaking: a) coating (magn. x450); b) subsurface layer (magn. x4500)

The microstructures of high-temperature affected gas turbine blades were also observed. This provided detailed information about changes in the microstructures of both the coating layer (alteration in the coating thickness) and in the parent material. Changes in material parameters, mainly modifications in the size and distribution of the γ′ phase, substantially affect mechanical properties of the material (Błachnio, 2009; Decker & Mihalisin, 1969; Dudziński, 1987; Mikułowski, 1997; Poznańska, 2000; Sims et al.,1987). Results of the examination of specimens subjected to soaking in the furnace at 1223 K and 1323 K are shown in Fig. 9 and Fig. 10, respectively.

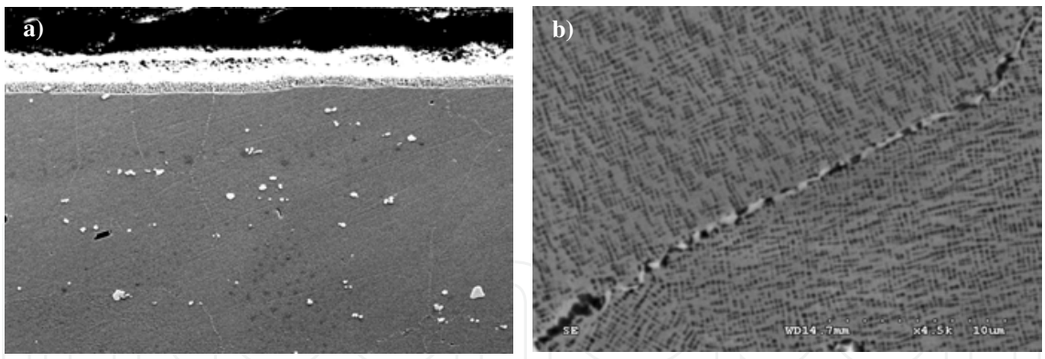

Fig. 9. Metallographic structure of the blade after soaking for 1 h at 1223 K: a) coating (magn. x450); b) subsurface layer (magn. x4500)

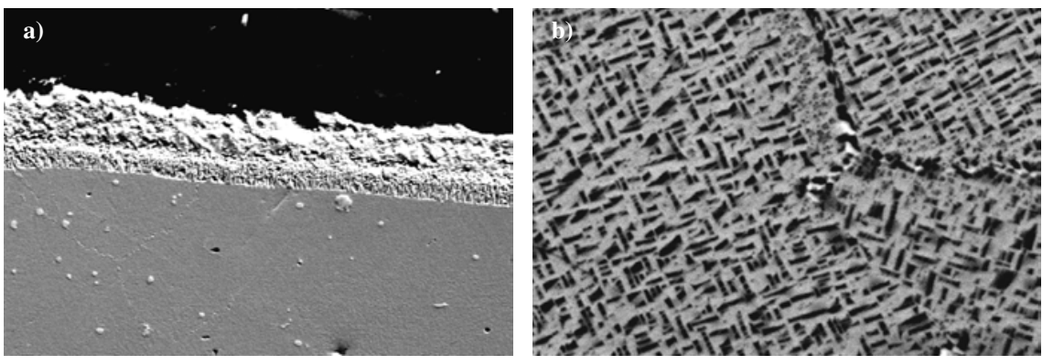

Fig. 10. Metallographic structure of the blade after soaking for 1 h at 1323 K: a) coating (magn. x450); b) subsurface layer (magn. x4500)

Relationship between the average thickness of the aluminium alloy coating and the soaking temperature of specimens is graphically shown in Fig. 11.

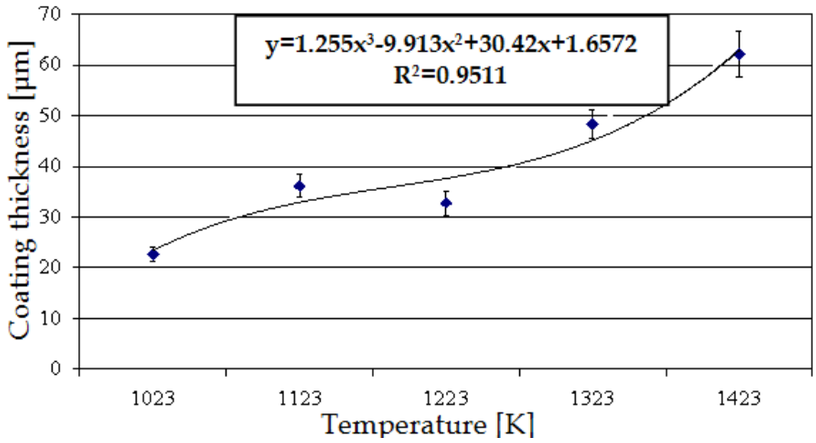

Fig. 11. Variation in the aluminium layer thickness against temperature

One can see the non-linear growth of the coating as a function of temperature, both nearby the surface and within the diffused layer. In consequence of that growth the layers exhibit less density (poorer tightness) and increased roughness that leads to amendments of the reflection parameters with regard to the incident light that illuminates the surface. In turn,

the graphic relationship between the average value of the γ′ strain hardening phase emissions and the heating temperatures for the EI 867-WD alloy is plotted in Fig. 12 and demonstrates the exponential nature, but can be approximated with a polynomial.

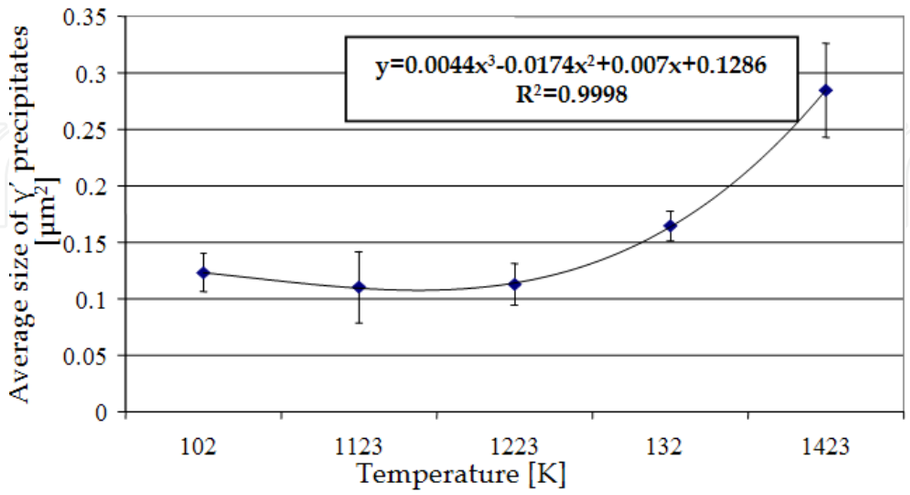

Fig. 12. Variation in γ′ particles of average size against temperature

Examination of the microstructure of blade specimens revealed that as early as at 1123 K there appeared the initial stage of coagulation of precipitates of the strengthening γ′ phase of relatively regular structure and very high density. As the temperature kept growing, the structure of the γ′ phase became less regular, and grain size was also growing. The initial period when cubic grains joined together to form plates started at 1223 K (Fig. 9b). It was found that as soon as the temperature reached 1323 K, the substantial growth and coagulation of γ′ phase precipitates followed; the γ′ precipitates adopted shapes of plates (Fig. 10b). Also, the number of particles was reduced but they were much larger than those at 1223 K.

To determine the blade serviceability (fit-for-use) threshold, it proved reasonable to develop a nomogram that presented correlation between the colour saturation in blade images and the size of the γ′ precipitates. The following assumptions resulting from the already described laboratory experiment were adopted:

1. Illumination – scattered white light;
2. No disturbing interferences of light reflected from other surfaces;
3. New gas turbine blades were used for tests;
4. Specimens cut out of blades were randomly selected and subjected to soaking (three pieces at a time) at five temperature values with the increment of 100 K, starting from the temperature of 1023 K;
5. Alteration in saturation (amplitudes of different wavelengths) of primary colours was adopted as the parameter that defines alterations in both chrominance and luminance of the examined surfaces.

To determine parameters that would enable description of the degree to which the microstructure of examined surfaces was changed (overheated), the technique of image analysis for the decomposition of primary colours, i.e. Red, Green and Blue (RGB) and shades of grey (parametric description of histograms) was employed. Due to the nature of the investigated phenomenon it was reasonable to only consider changes in the locations of

maximum saturation amplitudes (for individual histograms representing distributions of brightness of digital images (Bogdan, 2008) – Fig. 13.

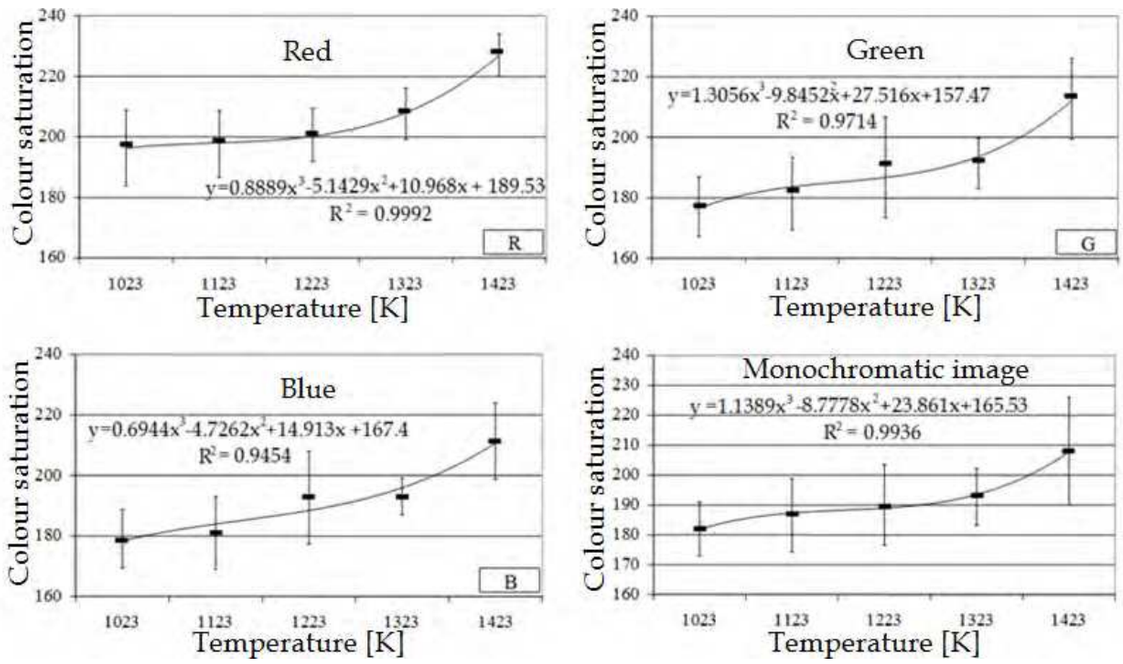

Fig. 13. Changes in locations of maximum amplitudes of saturation with RGB colours and shades of grey for various temperatures of specimen soaking

In order to find correlations between changes in colour of blade surfaces and the effect of temperature upon the blade microstructure the following nomograms were developed (Fig. 3.14 a, b) for the assessment of blade condition.

The assessment of blade condition is based on colour analysis of blade-surface images and is closely related with the material criterion (modification in the strengthening γ' phase , i.e. in both changes of shapes from cuboidal to plate-like and growth of precipitates), i.e. deterioration in high-temperature creep resistance and heat resistance after exceeding the temperature threshold of 1223 K. The nomogram that presents relationship between changes in colours of blade surface (in Red and greys) and temperature of blade soaking serves as the basis for the assessment of how much the microstructure of the EI 867-WD alloy was affected. When a mathematical description of the discussed phenomenon is introduced, the following regression curve equations result (the nomogram in Fig. 14b) for changes in:

- intensity of shades of grey (x_2):

$$x_2 = 0.2793e^{0.0189(z1-1150)} + 187.1 \tag{2}$$

  - the square of the correlation coefficient: R^2=0,9998
- average size of γ' precipitates (y_2):

$$y_2 = 0.0058e^{0.0142(z1-1150)} - 0.1 \tag{3}$$

  - the square of the correlation coefficient: R^2=0,9998

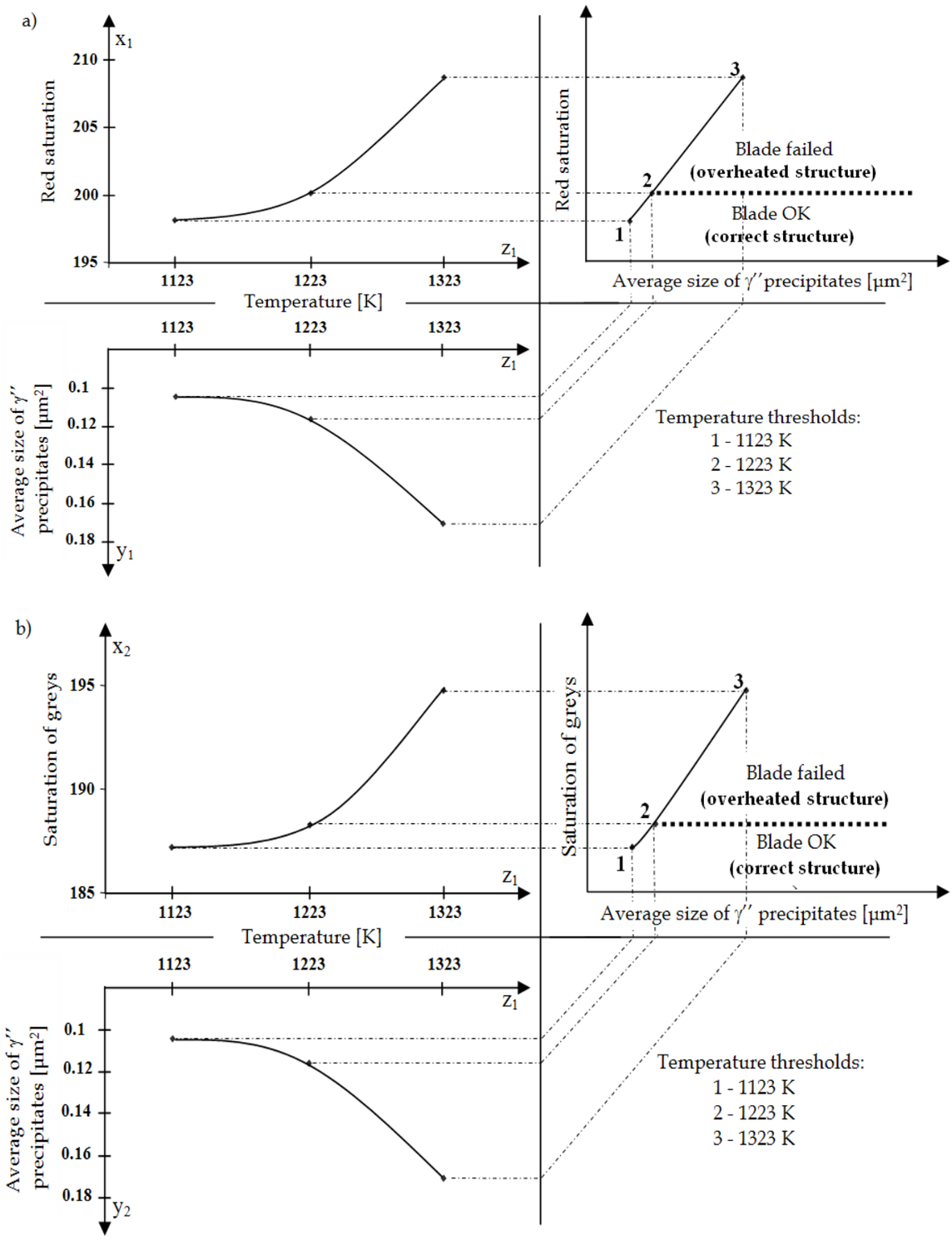

Fig. 14. Nomogram for the assessment of health of gas turbine blades on the basis of a) – alteration in Red saturation, b) – changes in shades of grey, as affected with changes in γ' precipitates at different temperatures of blade soaking

- average size of γ' precipitates as a function of greys intensity:

$$y_2 = 0.11512(x_2 - 187.1)^{0.7513} \tag{4}$$

where: z_1 – temperature [K].

Based on the foregoing functional relationship (equation 4) it is possible to assess condition of any blade (by its microstructure, i.e. the average size of the γ' precipitates) on the basis of the already calculated value of the degree of grey on the images of blade surfaces. Such an approach may prove useful, after taking account of disturbances and interferences, in formulating a mathematical model – the assessment of blade condition on the basis of changes in colours.

High temperature not only entails both changes in thickness of the aluminium coating (variable light-reflecting area) and modifications in the structure of γ' phase. In practice, alterations of the aluminium coating lead to variations of the luminance and chrominance of the surface that is recorded by the optoelectronic system furnished with the light-sensitive detector, i.e. the CCD matrix (digital images). The investigated microstructure of the subsurface layer reflects transformation of the EI 867-WD alloy and serves as the evidence for overheating of its structure (Fig. 10b, 11) after heating of the blade specimens at temperatures exceeding 1223K. When assuming the material criterion, i.e. size alterations of emissions for the γ' phase, as a criterion that is decisive for approval of blades for further operation, it is possible to find out the operability threshold that would qualify or disqualify blades for further use.

The soaking of blade specimens leads to structural changes in the superalloy. At the same time, roughness changes and thickness of the aluminum coating increases (Fig. 11). Changes in the coating's parameters (roughness, thickness) influence capability of the surface to reflect a luminous flux and its spectral composition (saturation in RGB). In addition, investigation into the chemical composition revealed that the soaking results in modification of the percentage weight-in-weight concentration of elements that make up the coating – Table 1. A substantial difference can be noted mainly in the content of such elements as W, Mo, Ni and Al.

Soaking temperature [K]	Elements by weight [%]							
	O	Al	Cr	Fe	Co	Ni	Mo	W
1423[K]	9.89	9.66	11.73	0.68	4.50	41.12	11.73	10.58
1023[K]	6.26	2.94	10.31	0.84	5.44	57.27	5.66	7.28

Table 1. Chemical composition of the aluminium coating subjected to soaking at 1023 and 1423 [K]

These are also the factors that affect conditions of reflecting the luminous flux to result in changes of colours of blade surfaces for particular soaking temperatures.

3. Diagnostic examination of operated stator vanes

The research program assumed examination of gas-turbine stator vanes of an aircraft jet engine. The vanes were manufactured of the ŻS6K alloy. The alloy in question has been strengthened with cubical γ' phase particles, the content of which amounts to approx. 64%. It is classified to the group of cast alloys. Figures below (Figs 15, 16 and 17) present exemplary sets of recorded images of turbine vanes with different degrees of overheating (according to the already applied classification of vane condition).

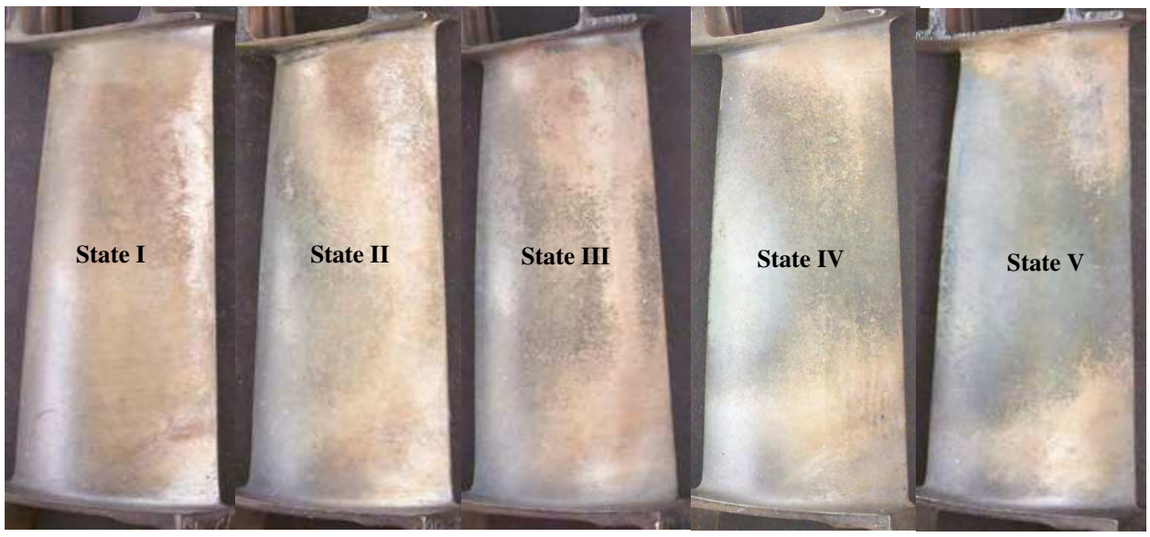

Fig. 15. Recording of vane surface images with a photo camera

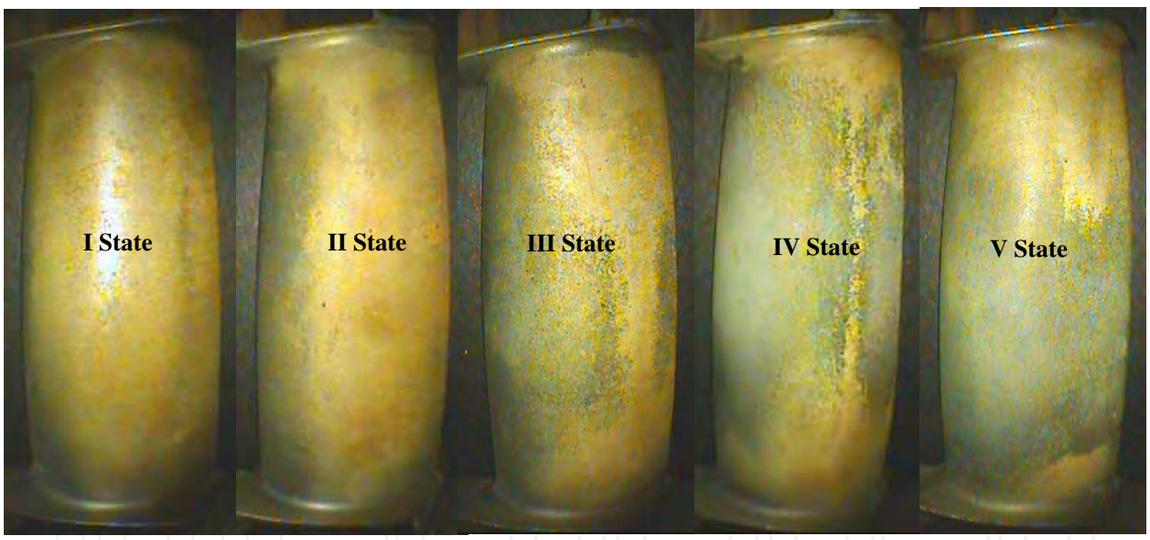

Fig. 16. Recording of vane surface images with a videoscope No. 1

Differences in colours of recorded images of turbine vanes surfaces result from properties of optoelectronic systems (chiefly, the CCD matrix) and variations in illumination (type of light) used in particular instruments. When images were taken with a photo camera, the illuminating light was uniformly scattered on entire surfaces of vanes, whilst the light emitted by videoguides was of focused nature.

The analysis of the collected vane-surface images in terms of estimation of changes in colours and shades of grey resulted in finding out the following changes in locations of maximum amplitudes for particular component colours:

- for images recorded with the digital photo camera (Fig. 18):
- for images recorded with use of the videoscope No 1(Fig. 19):

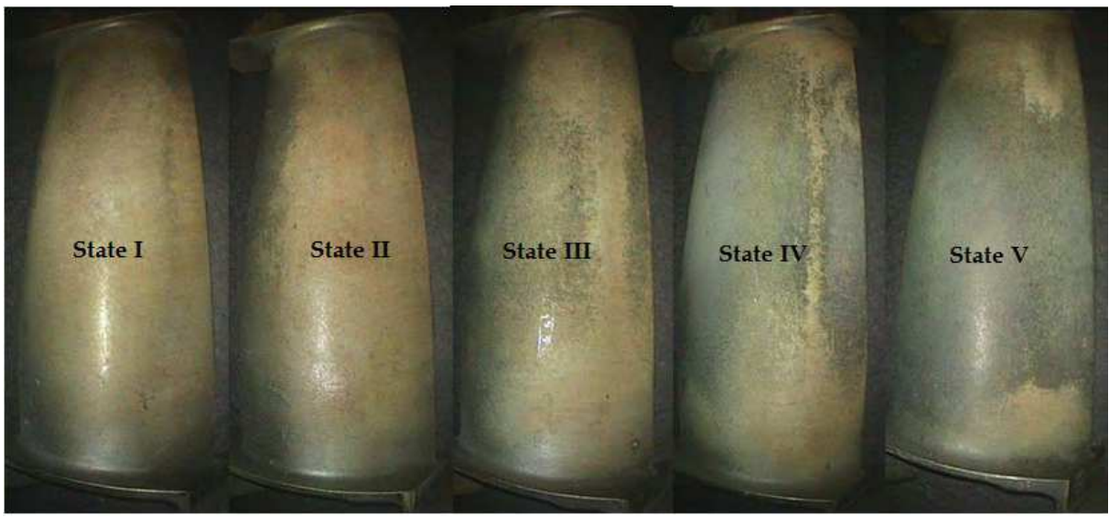

Fig. 17. Recording of vane surface images with a videoscope No. 2

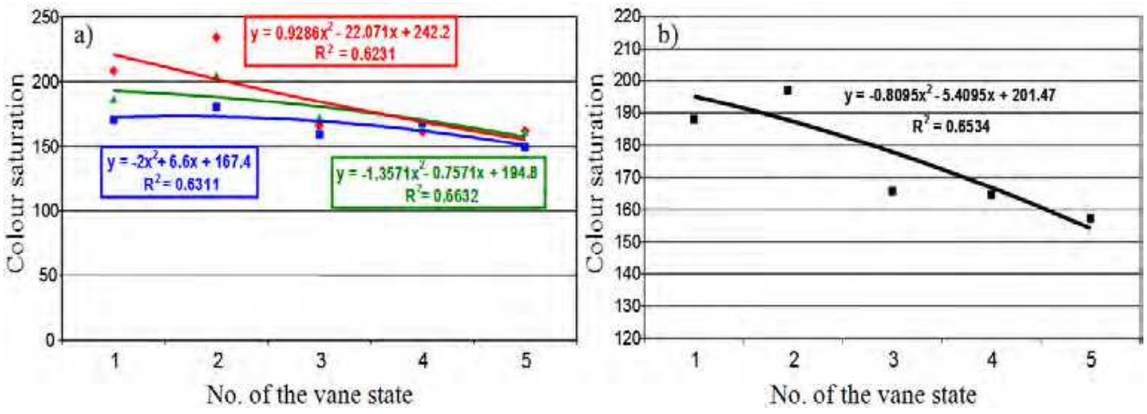

Fig. 18. Dislocation of the maximum saturation amplitudes of the image for various states of vanes: a) RGB components; b) grey shades

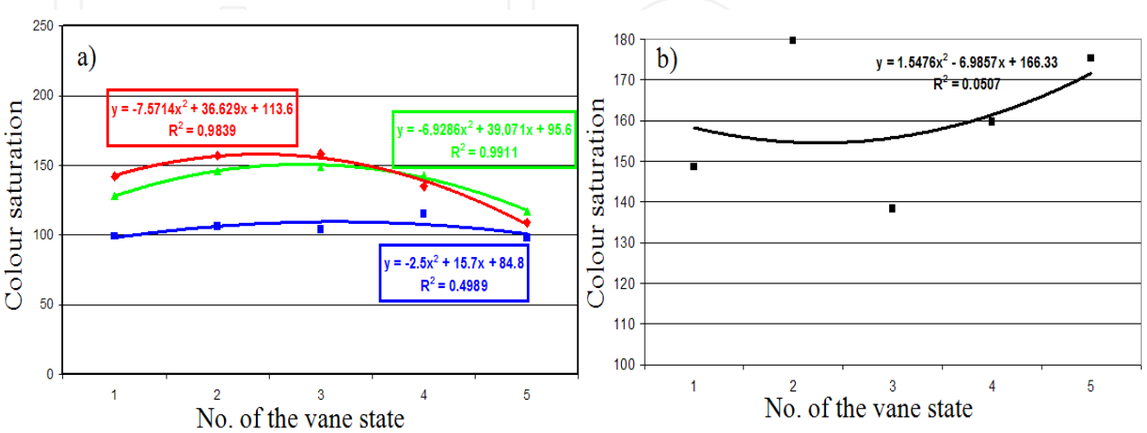

Fig. 19. Changes in locations of maximum amplitudes of image saturation for various states of vanes: a) RGB components; b) shades of grey

- for images recorded with the videoscope No 2 (Fig. 20)

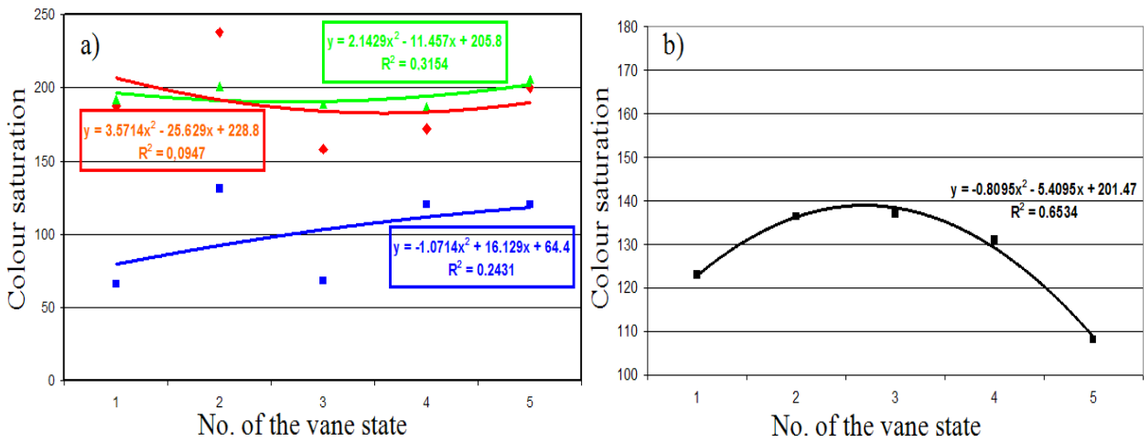

Fig. 20. Changes in locations of maximum amplitudes of image saturation for various states of vanes: a) RGB components; b) shades of grey

The curves (trend lines) demonstrate correlation coefficients much worse than those obtained from laboratory tests. It has been caused by the forms of histograms (the colour range of images is wider). However, for images recorded with a digital photo camera the surface colour represents changes due to the exposure of the material to high temperature (Fig. 18). To recognise microstructures of vanes that had already been in operation further metallographic examination was carried out under laboratory conditions. As in the experiment with new blades subjected to soaking, the examination was carried out using metallographic microsections. Two microscopes were used: optical and scanning (SEM) ones. After long-time operation the vanes manufactured of the ŻS6K alloy demonstrated different health conditions. On the basis of metallographic examination (Bogdan, 2009) it was found that initially, after some time of operation, the vane coating suffers no degradation and its thickness is nearly the same as that of a new vane. Later on, it starts to suffer swelling, which after a pretty short time may result in crack nucleation due to thermal fatigue. Since the working agent (exhaust gas) of high kinetic energy keeps affecting the vane material (the surface layer), successive changes in thickness of this layer follow. The coating is getting thinner and thinner and, therefore, loses its protective properties. Consequently, temperature of vane material grows by approx. 100 K and it is no longer protected against chemical effect of the exhaust gas. The vane becomes much more vulnerable to the exhaust gas, which results in complete deterioration of the protective coating or even the parent material. Furthermore, morphology of the γ' phase has been found to prove that after critical temperature is exceeded the alloy becomes overheated. The turbine vane cannot be then considered serviceable (fit for use). Therefore, on the basis of findings of vane microstructure analysis it is possible to state that vane no. 1 (i.e. State I) exhibits correct microstructure, whilst the structure of vane no. 5 (i.e. State V) is overheated. When these results are compared to those of the analysis of blade surface images, it is possible to infer that vanes no. 1 and 2 are in sound condition, since parameters of image properties are comparable. On the other hand, vanes no. 4 and 5 are overheated, as values calculated from the histogram (as well as from the co-occurrence matrix) are much different from those for earlier discussed items. Thus, it is feasible to demonstrate correlation between

images of surfaces of turbine vanes in service and condition of microstructures of these vanes made of the ŻS6K alloy, covered with protective coatings. Metallographic examination of vanes in service has also allowed of the development of two methods for scanning surface images, i.e. one based on colour profiles, and another based on the value of plane. The subsequent stages of the first method are listed below:

- acquisition of images with a digital photo camera (laboratory conditions) or two videoscopes (real operating conditions),
- cutting of vane no. 5 (according to the earlier assessment, considered as overheated);
- plotting of averaged colour profiles down the cutting lines with account taken of the width of cutting (the model adopted to represent digital images – the RGB model);
- determination of variations in the coating thickness and changes in both sizes of precipitates and distribution of the strengthening γ' phase (the SEM microscope – the computer-aided analysis of metallographic images);
- on the basis of alterations in microstructure parameters - determination of colour lines that represent overheated and non-overheated structures;
- scanning of images of conditions I - V against the selected colour profiles.

According to the already applied classification, the fifth condition (state) denotes an overheated vane. To verify this judgement, further metallographic examination was carried out along two cutting lines. The changes in the coating thickness (on the aluminium matrix) were measured and changes in size of precipitates and shape of the strengthening γ' phase (the scanning (SEM) microscope, the computer-aided analysis of metallographic images). Alterations in these two parameters are of crucial importance for the heat resistance and high-temperature creep resistance of turbine vanes. Thus, it was possible to plot an averaged colour profile (taking account of the width of cutting) that represents an overheated structure (the selected range along line *1* – Figs 21a, b, and a non-overheated structure (the selected range along line *2* – Figs 22 a, b).

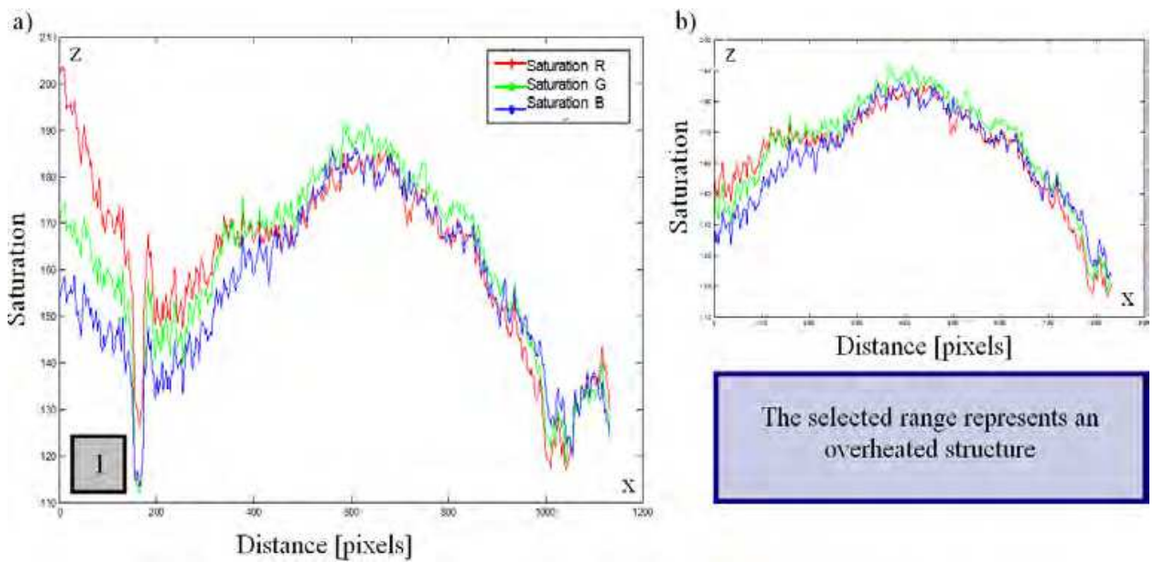

Fig. 21. Averaged RGB profiles: a) along line no. 1 – parallel to the normal direction (KN); b) the selected range that represents an overheated structure

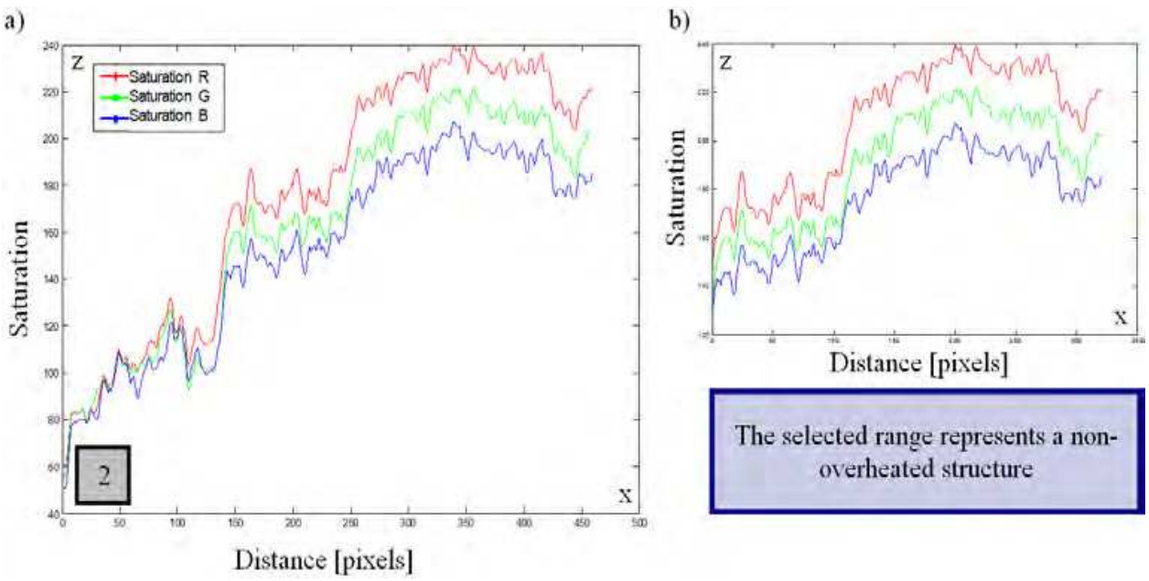

Fig. 22. Averaged RGB profiles: a) along the line no. 2 – perpendicular to the normal direction (KN); b) the selected range that represents a non-overheated structure

Next, on the basis of two ranges of colour profiles (Fig. 21b, Fig. 22b) each component (one pixel after another) of surfaces from states (I-V) of vanes was examined with regard to the occurrence of colour dots (RGB) that correspond to either overheated or non-overheated structure. Finally, the ratio of the overheated surface area to the overall surface area of the vane was obtained (Fig. 23).

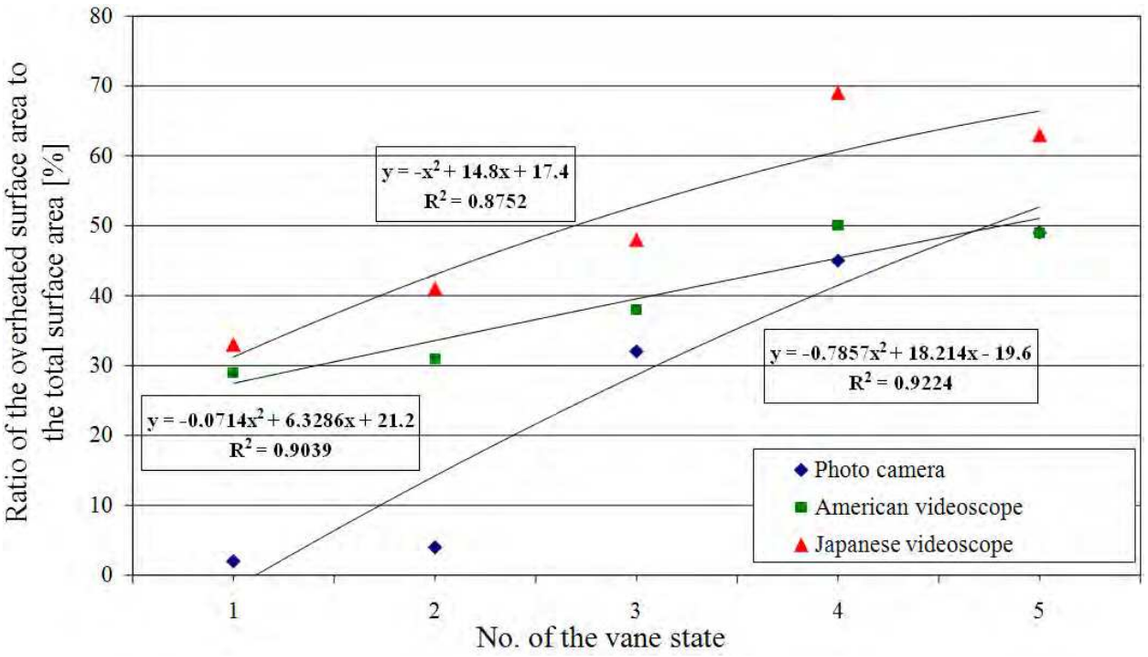

Fig. 23. Ratio of the overheated surface area to the total surface area for particular states of the vane – detection of images with a photo camera and two types of videoscopes

In the second method (Bogdan & Błachnio, 2009), the surface colour of the State V vane (the overheated structure according to metallographic examination) was assumed the overheating criterion. Based on the developed histograms, the criterion threshold was determined, where the threshold value was calculated on the basis of saturation (location of the maximum amplitude) for individual RGB components (R+G+B/3=162). The criteria threshold (value of the plane) was then referred to 3-D distributions of colours on surfaces of individual vanes from states I to V. Points with values below the determined plane were deemed the overheated surface points (pixels). Instances of estimating overheated surfaces for vanes from states I and V have been graphically shown in Figs 24 and Fig. 25, with images recorded with the digital photo camera. To make the image more clear, the Cartesian coordinate system was adopted (where: *x, y* – dimensions of the vane image in pixels, *z* – RGB saturation).

The dashed lines (Fig. 24a, Fig. 25a) represent the non-uniform effect of temperature on the vanes under examination, caused by faulty operation of injectors – irregularities in the combustion process inside the combustion chamber.

The area of overheated surface (the set of image points) extends as condition of vanes deteriorates - Fig. 24c, Fig. 25c. Introduction of the threshold plane (criterion of vane material overheating) in the 3-D charts of RGB distribution in images of surfaces of the turbine component under examination allows of the determination of the ratio of the overheated surface to the overall surface.(Fig. 26).

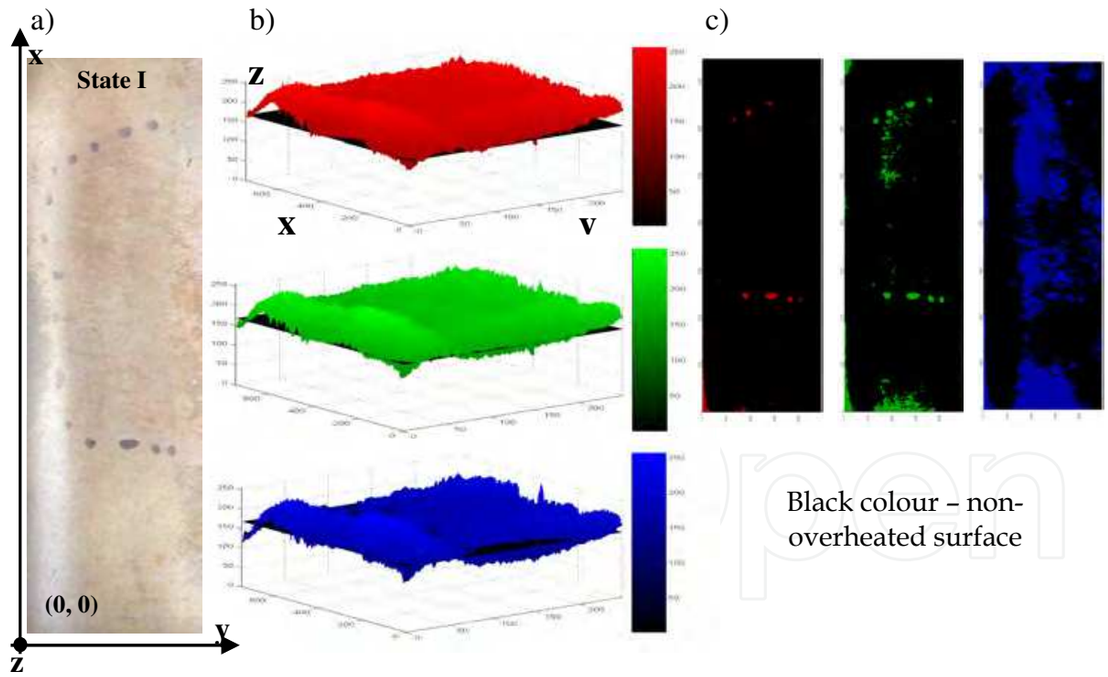

Fig. 24. Vane representing State I: a) surface image; b) 3-D distribution of RGB primary colours; c) vane surface viewed from below – the result of introduction of the criterion plane

The best results were gained for images of vane surfaces recorded under laboratory conditions with the digital photo camera. On the basis of the plotted curves (Fig. 23, Fig. 26 and Fig. 27) one can conclude that changes in colours of vane surfaces reflect health/maintenance status of the examined turbine components. Application of one of the

two proposed methods , or both of them, of scanning the vane surfaces, i.e. the method based on the already determined colour.

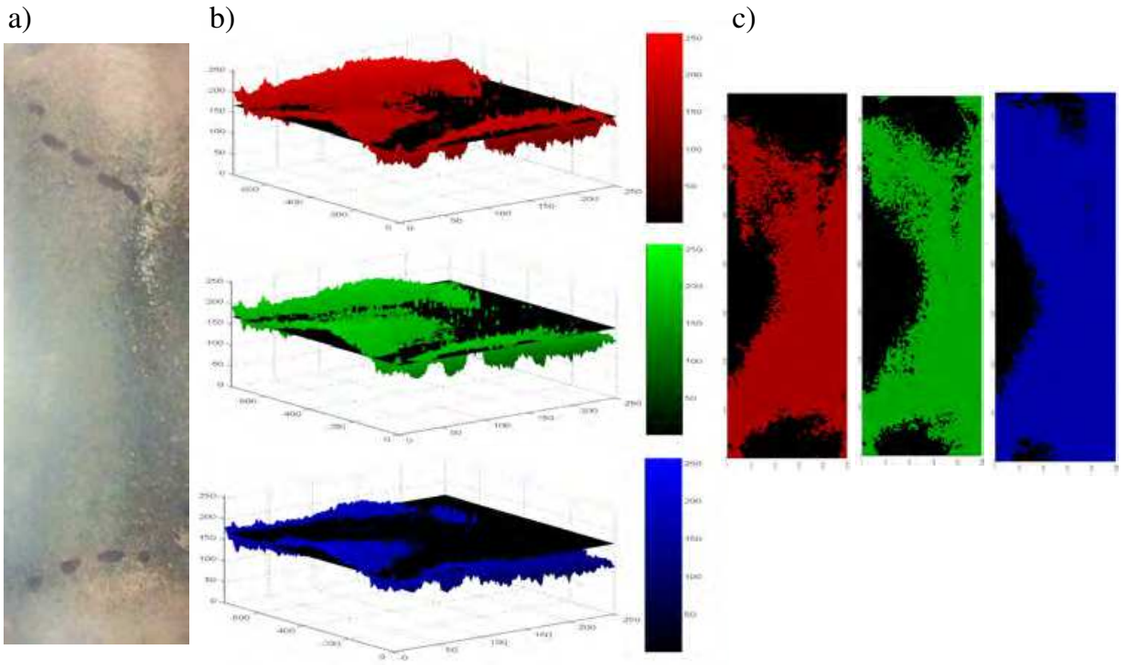

Fig. 25. Vane representing State V: a) surface image; b) 3-D distribution of RGB primary colours; c) vane surface viewed from below – the result of introduction of the criterion plane

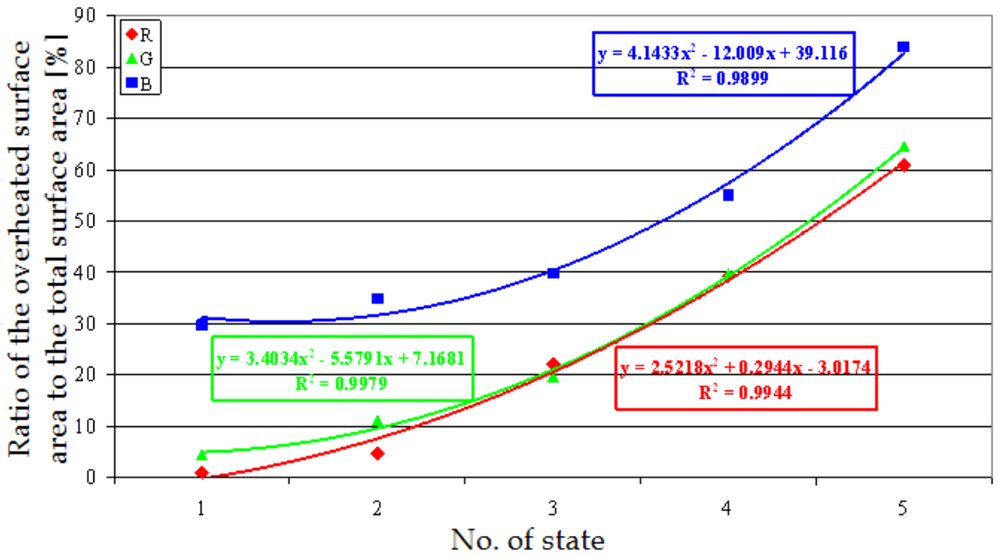

Fig. 26. Ratio of the overheated surface area to the overall surface area –images recorded with a digital photo camera

Identical relationships were determined for images recorded with two videoscopes (Fig. 27).

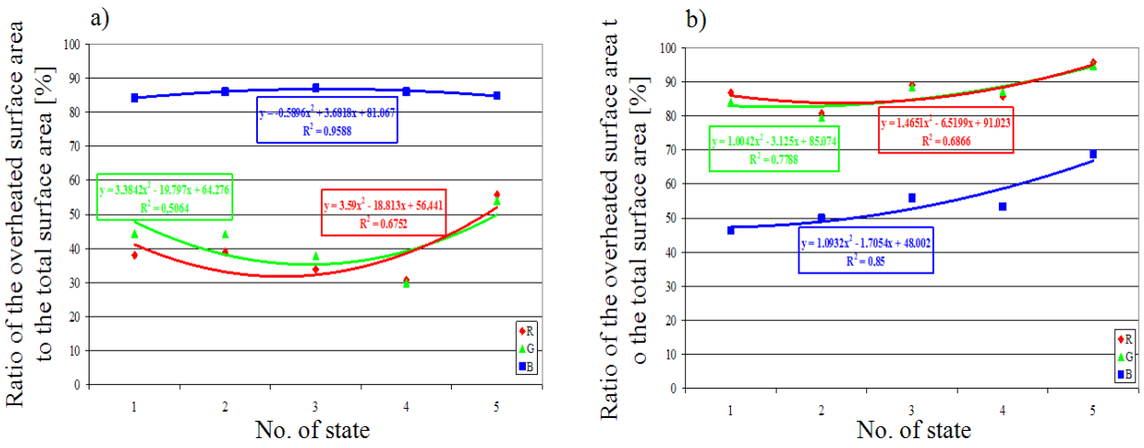

Fig. 27. Ratio of the overheated surface area to the overall surface area, a) images recorded with videoscope No. 1, b) images recorded with videoscope No. 2

profiles that respectively represent the correct and the overheated structures, and the method of the criterion plane improves likelihood (objectivity) of the assessment of the vane condition. The computer-aided acquisition of images together with dedicated software for image recognition will improve the process of the assessment itself and contribute to more trustworthy analyses than it used to be in past. Percentage differences between particular states result from the applied type of light and the way of illuminating the examined vanes. Under laboratory conditions only white scattered light was used, whilst videoscopes incorporate sources of light focused in other colour. Capability to recognize and record colours may also be different due to light-sensitive CCD matrices installed in various detection instruments. Nevertheless, it must be noted here that the application of endoscopes (videoscopes) for the acquisition of images may be used to track (monitor) changes in vane condition (development of failures, health/maintenance status of components under examination) in the course of periodical inspections with no need to dismantle the entire gas turbine.

4. Application of neural networks in diagnostics of vanes

The subsequent paragraphs present the opportunities to apply artificial neural networks to diagnostic examination of vanes, both new ones (after heating) and those that have already been in operation. The major objective was to develop such a neural network that would be capable of diagnosing the technical status of the turbine component under test on the basis of parameters for images of their surfaces. The metallographic examinations were carried out to assess technical condition of the turbine component in question. Alterations of the metal structure were taken into account, such as thickness alteration of the protective aluminium coating and changes in average size of emissions for the γ′ phase (the strain hardening phase of the alloy, which is the phase that predominantly decides on creep resistance properties). The metallographic examination made it possible to classify vanes according to their technical condition. Fig. 28 explains an example of such classification of vanes that demonstrate various technical conditions (wear degree) – the material criterion.
On the basis of conclusions related to assessment of the overheating degree (vanes applicable and inapplicable for further operation) and drawn from microstructure

examinations, the pattern images were adopted for vane surfaces representing various degrees of deterioration (the neuronal pattern classification). Nowadays a great number of supervised networks are available, although, in fact, they are merely options or variants of a limited number of models. For this study only models that offered the best results (verification of classification correctness on a set of test benchmarks) were taken into account, i.e. the Multi-Layer Perceptron (MLP) and the network with Radial Basis Function (RBF). Examples for structures of such networks are shown in Fig. 29. Each of the networks is made up of three layers (one input layer, one hidden and one output) with the same number of neurons per each layer.

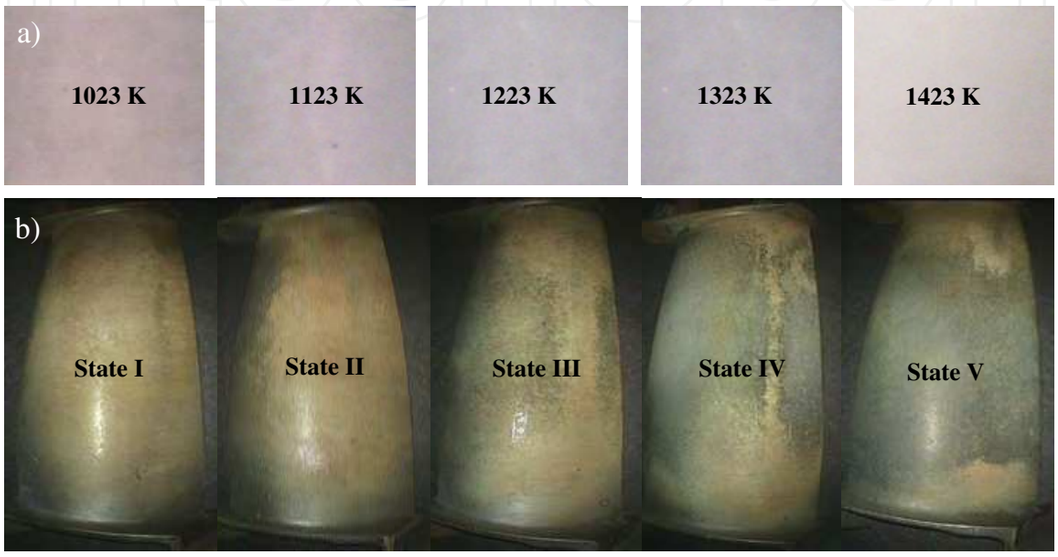

Fig. 28. Acquisition of surface images of blades/vanes: a) heated (images recorded with a photo camera); b) operated (images recorded with the videoscope no. 2 Three-state)

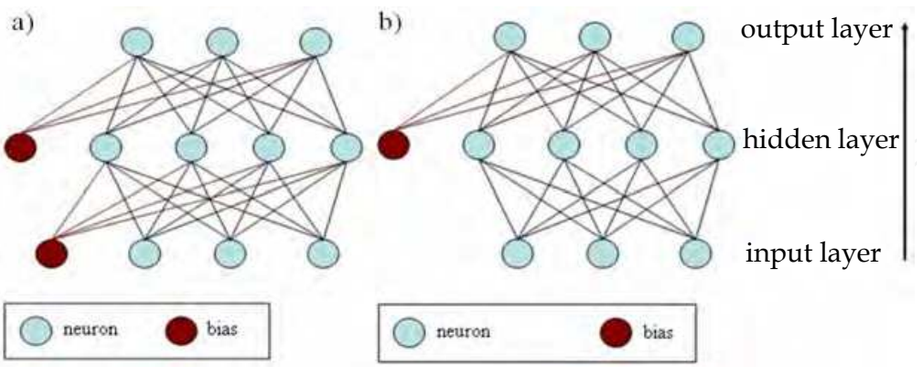

Fig. 29. Diagram of the network: a) the Multi-Layer Perceptron (MLP); b) the Radial Basis Function (RBF) network

For the perceptron network the neurons are deployed exclusively between subsequent layers and signals propagate to only one direction (the unidirectional network). The number of hidden layers is actually unlimited, but it has been proved that two layers are perfectly sufficient for any transformation of input data into output ones. Learning of networks of

such a type is usually carried out in the mode with a teacher, by means of the gradient method of the first of second order, by minimization of the error function. In case of a multi-layer perceptron the excitation level of a neuron is the weighted sum of inputs (plus the threshold value that is added as a bias). When a auxiliary bias input is added to a neuron the networks acquires higher ability to learn owing to the possibility to shift the activation threshold depending on the weight of the bias input. For Radial Basis Function (RBF) networks the bias input is added exclusively to neurons within the output layer. Moreover, the network type that uses the radial basis functions has usually one hidden layer that comprises neurons with a radial function of activation. Output neurons usually represent the weighted sum of signals coming from radial neurons deployed in the hidden layer. Learning of that type of networks consists in selection of weight coefficients for the output layer and parameters of the Gaussian radial basis functions.

The objective of the newly designed neuronal classifier was to develop a (computer-aided) method that would enable to recognize technical condition of a specific vane on the basis of its surface image (its properties). Two following cases were considered:

1. Two-state classification (for blades and operated vanes):
   - - class 1: operable status (non-overheated blade/vane);
   - - class 2: inoperable status (overheated blade/vane);
2. 2. Three-state classification (only for operated vanes):
   - - class 1: operable status (non-overheated vane);
   - - class 2: partly operable status (the vane suspected to be overheated);
   - - class 3: inoperable status (overheated vane);

The first phase of the development consisted in acquisition of data that were subsequently used to model the network (input data) and for further tests (verification of ability to correct classification). In order to reduce the amount of information, the colour images were converted into black and white ones (8 bit encoding of grey shades, 0-255). Then 10 input parameters were selected (image parameters). Six first parameters (P1-P6) describe the histogram, i.e. distribution of pixel brightness. Four subsequent parameters (P7-P10) were found out on the basis of the co-occurrence matrix (for the distance of 1 and angle of 0^o) – Table 2.

Designation	Specification
P1	value of maximum saturation
P2	value of average brightness
P3	fluctuation of brightness distribution
P4	histogram skewness
P5	histogram kurtosis
P6	histogram excess
P7	contrast
P8	correlation
P9	energy
P10	homogeneity

Table 2. Input data – the feature vector

The preliminary metallographic investigations (the material criterion) made it possible to state that the new blades heated at the temperatures of 1023K and 1123K exhibit correct metallographic structure whilst the ones that are heated at 1323K or 1423K are overheated (Fig. 28a). In case of vanes that have already been in operation, the vanes of correct metallographic structure are those of the I and II state, whilst overheated vanes are from the IV and V state (Fig. 28b). Owing to such classification it was possible to embark on the network modelling. The modelling phases were the following:

1. Standardization of data and encoding of outputs (classes);
2. Subdivision of data into the learning pattern and test pattern (at the shares of 50% to 50%);
3. Determination of parameters for the neuronal network, such as minimum and maximum number of hidden layers (for MLP and RBF networks), types of activation functions, both for hidden and output neurons (for the MLP network), minimum and maximum values for reduction of weight coefficients, for both hidden and output neurons (for the MLP network).

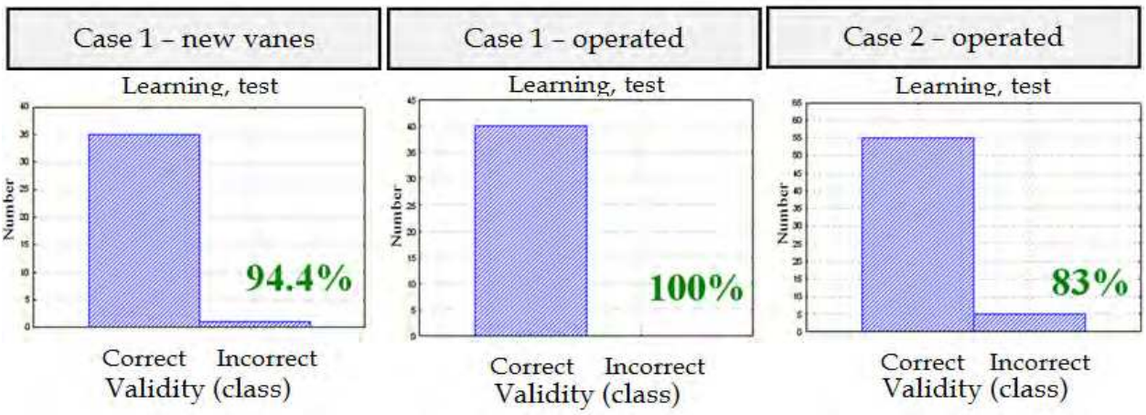

Fig. 30. Comparison between validity of classification

The network was subjected to the learning process with use of the set of input data. As a result of the simulation process, both in the learning and the test modes, the optimum models of neuronal networks were developed for each case (two-state and three-state classifications). It was confirmed that neuronal networks offer a useful tool to assess status of vanes, both new ones (after heating) and those that have already been in operation (Fig. 30).

The developed neural classification models (networks with a defined architecture) make it possible to determine technical condition of vanes on the basis of features (parameters) attributable to their images with satisfying dependability. The additional advantage of such an approach is the possibility to carry out the diagnosis process under conditions of continuous operation of the turbine (with no need to have it dismantled), where images of specific parts of turbines are acquired with use of a videoscope and then transmitted to the control computer, where the dedicated software extracts the required features (parameters) of the images. Finally, the 'modelled network' (well learned) indicates whether the vane is suitable for further operation. The three-state classification enhances the diagnostic process by the possibility of approving a vane for further, but supervised operation i.e. until the date of scheduled assessment.

5. The thermographic method for technical condition assessment of gas turbine vanes and blades

5.1 The passive infrared thermography

Thermographic methods represent relatively new but rapidly developing approach to non-destructive diagnostic examination of materials. Thermography not only enables measurements of temperature, but also determination of temperature distribution on the basis of the detection of infrared radiation emitted by examined surfaces. In the literature, the thermography is frequently referred to as 'thermovision' (Oliferuk, 2008).

For the entire spectral range, power of electromagnetic (EM) radiation emitted by surfaces of materials depends on temperature of a given surface, and peaks of the radiation of power fall within the infrared (IR) range. The infrared radiation fits within the range of electromagnetic waves from 0.75 to 100 μm, i.e. remains outside the very narrow interval of light visible to the human eye (0.4 to 0.7 μm). With a suitable infrared detector available, and with both the relationship between radiation power and temperature of the emitting surface and dependencies of the signal at the detector output on this power known, it is possible to determine temperature of the surface in a non-contact way. The infrared thermography method based on detection of infrared radiation (like all non-destructive testing methods) can be split into passive and active techniques. A research method based on detection of infrared radiation without the need to additionally stimulate the examined object (supplying with energy) is referred to as the passive infrared thermography.

Emissivity of materials is expressed by the following formula (Oliferuk, 2008):

$$E(\lambda, T) = \frac{dW_e}{d\lambda} \tag{5}$$

where: dW_e is the energy of electromagnetic radiation emitted in a time unit by a unit of surface of the material within the range of wavelengths λ to $\lambda+d\lambda$.

Among a number of fields, the thermographic method is also widely applied to technical diagnostics, owing to advanced thermographic systems offering the possibility of determining the temperature distribution on the examined surface with temperature resolution better than 0.1K. The range of applications of the method includes inspection of electric circuits and systems, integrated circuits, mating parts of machinery and structures, civil engineering, power engineering, diagnostics of high-temperature structures.

The diagnosing of gas turbines with the passive thermographic techniques consists in the recording of images of temperature distribution of turbine components at the exhaust nozzle's outlet. The starting point for any efforts intended to assess condition of the turbine components is development of pattern thermograms for correct operation of the turbine. Then, in the course of routine inspection carried out during regular operation of the turbine components the generated thermograms are compared with available patterns. If only a slight anomaly appears, it is considered a signal to initiate searching for any reason for the discrepancies. Owing to such an approach, it is possible to detect defects such as erosion of the turbine, failures to vanes/blades, incorrect operation of the combustion chamber, etc., i.e. ones hard to detect with other non-destructive inspection methods (Korczewski, 2008; Lewitowicz, 2008)

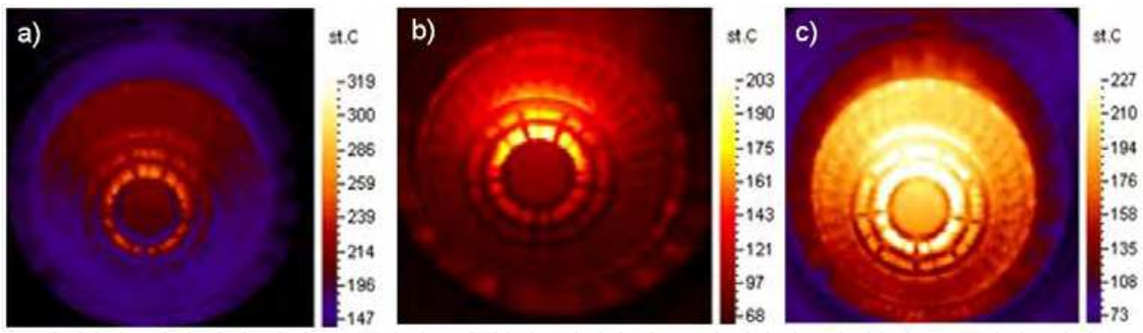

Fig. 31. Infrared radiation emitted by the turbine during the engine start-up: a) – start-up, b) – pre-heat, c) – operation (Haralick R. M. et al, 1973)

5.2 Active infrared thermography

The essence of the active infrared thermography consists in determination of thermal response of the examined material to stimulation by means of an external pulse of heat. Nowadays, research into the application of the active infrared thermography to detection of defects in surface layers of materials experience flourishing development. When a specific quantum of heat is delivered to the material surface, e.g. in the form of a heat pulse, the temperature of the material surface will be changing rapidly after the pulse termination. Owing to thermal diffusion, a thermal front moves deeper into the material. The presence of areas that differ in thermal properties (i.e with defects) from defect-free areas provokes some change in the rate of diffusion.

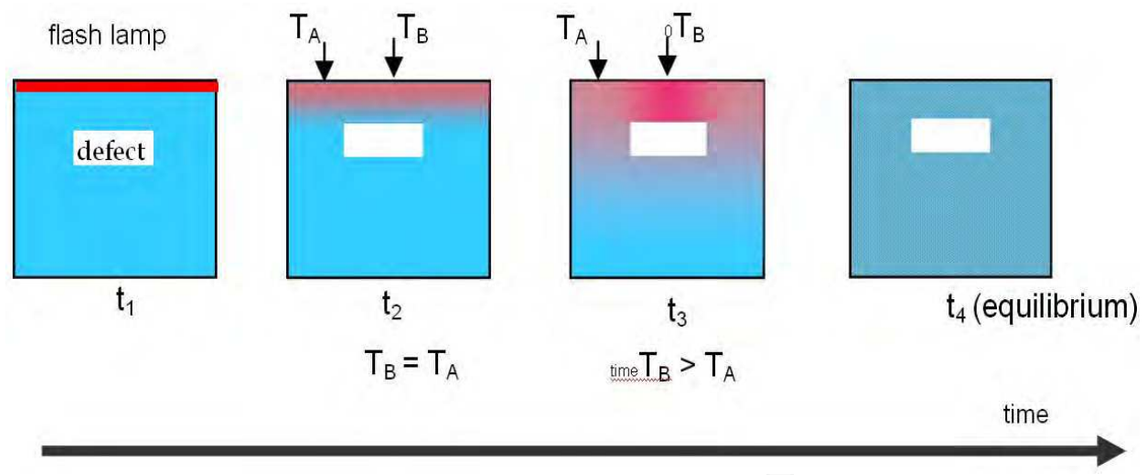

Fig. 32. Change in temperature of the specimen's surface after stimulation with an external heat pulse (Thermal Wave Imaging, Inc., 2009)

Thus, the monitoring of the temperature field on the surface of a specimen subjected to cooling provides capability to show locations of defects. The simpliest method of processing the signal recorded with an infrared thermograph while cooling the examined surface down consists in calculating the temperature contrast. The contrast is defined by the following relationship (Oliferuk, 2008):

$$C_a(t) = T_p(t) - T_{pj}(t), \tag{6}$$

where: $C_a(t)$ – absolute contrast, $T_p(t)$ – temperature at any point of surface of the examined material, $T_{pj}(t)$ – temperature at the point of surface above the homogeneous (i.e. defect-free) material.

Values of the absolute contrast are higher than zero at the points of surface right above the area of the material where a discontinuity exists. Depending on the stimulation method, several types of the active thermography are distinguished, namely: the pulsed thermography, the lock-in thermography with modulated heating and the pulsed phase thermography (Maldague, 2001; Thermal Wave Imaging, Inc., 2009).

The pulsed thermography is deemed as a rather simple variation of the active thermography and consists in the determination and analysis of temperature distribution on the examined surface when the surface is being cooled down after having been uniformly heated with a thermal pulse (Fig. 33). For the one-dimensional model and homogenous material, the equation that describes the change in temperature while the surface is being cooled down after heating with a short thermal pulse takes the following form (Oliferuk, 2008; Luikov, 1969):

$$T(t) - T(0) \approx Q\alpha^{-\frac{1}{2}} t^{-\frac{1}{2}} \tag{7}$$

where: Q stands for energy of the thermal pulse per each surface unit, t - time when the surface is being cooled down, α- thermal diffusivity, $T(0)$ – temperature at a selected point or on the area of the heated surface, just after termination of the thermal pulse and $T(t)$ - temperature at any moment of the cooling process.

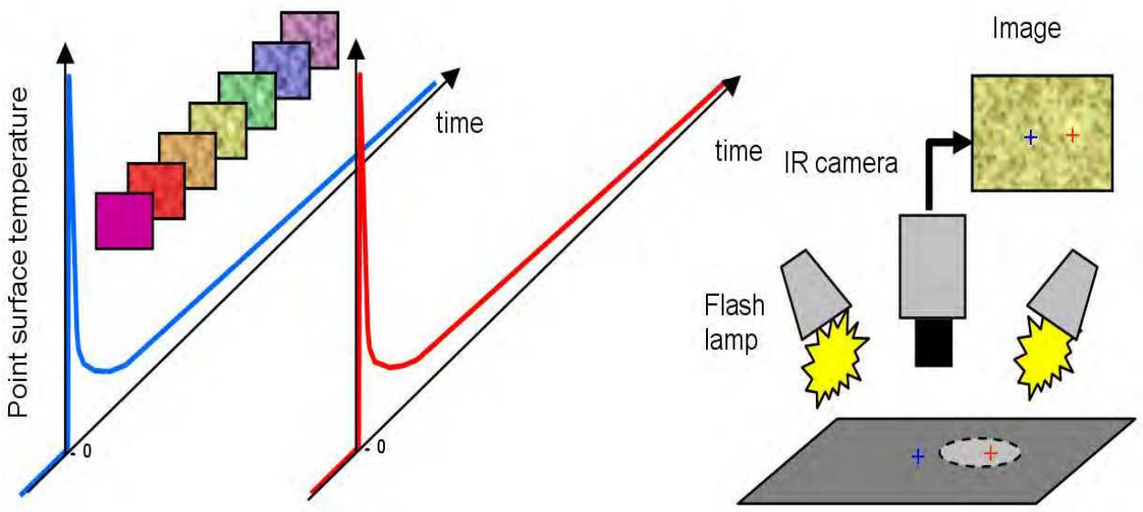

Fig. 33. Diagram to explain the application of pulse thermography (Thermal Wave Imaging, Inc., 2009)

When any flaws occur in the examined material, diffusion rates are reduced, which makes the temperature of the area of the surface above the flaw be different from the temperature of the area of the surface below with no defect – the nature of the foregoing interrelationship changes. Various physical properties of materials facilitate specialized diagnostic examination, e.g. determination of materials health, constitution of their structures, or identification of the material under examination, etc. The pulsed thermography enables one to distinguish temperature values in the course of cooling the specimen's surface down after

preliminary treatment with a thermal pulse. The acquired information contained in thermal response from the examined surfaces enables detection of other types or grades of materials present in the specimen (Fig. 34)
Obviously, this method (as other ones) has its limitations, since it enables one to detect flaws only in subsurface layers of materials due to the fact that the temperature contrast rapidly fades out with the depth of penetration. The research work has demonstrated that flaws located in deeper layers reveal themselves, however, later and with a poorer contrast. Time $t_{d,}$ from the termination of the stimulating pulse to the flaw revealing itself is proportional to the square of the flaw depth z (Oliferuk, 2008):

$$t_d \approx \frac{z^2}{\alpha} \tag{8}$$

whilst contrast C substantially fades as the depth of flaw increases (Oliferuk, 2008):

$$C \approx \frac{1}{z^3} \tag{9}$$

The experiments have also demonstrated that the radius of the smallest detected flaw must be at least twice as high as the depth where the flaw is located.

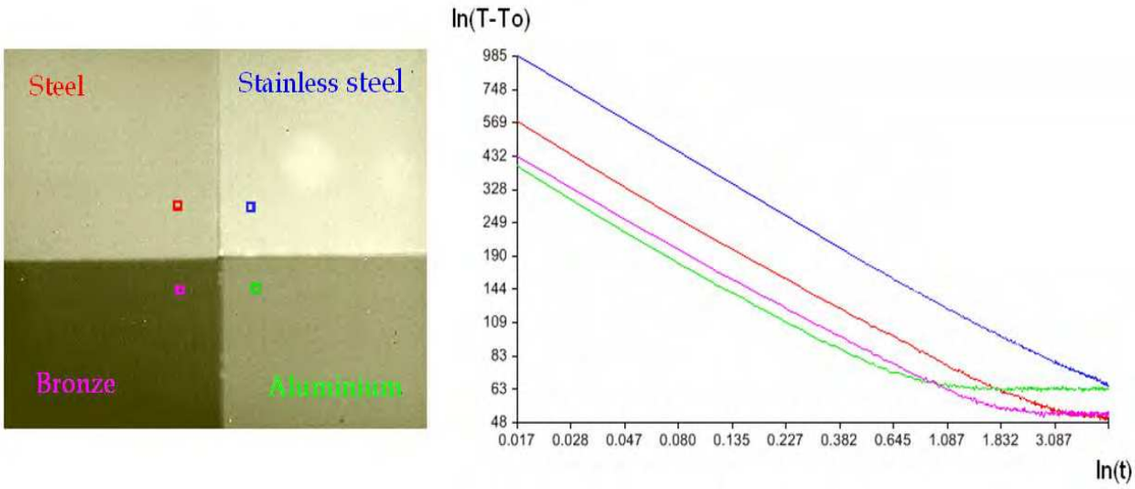

Fig. 34. Thermal response to a thermal pulse for selected grades of materials (Thermal Wave Imaging, Inc., 2009)

The drawback of the pulse thermography is that the examined surface has to meet requirements of the emission homogeneity, which is associated with the need to coat it before examination with a homogenous film, i.e. graphite.
On the other hand, methods based on another parameter, i.e. on the phase of the thermal wave, are free of the mentioned drawback. This is why these methods are widely applied in the active lock-in thermography with modulated heating and in the pulsed phase thermography (Oliferuk, 2008). The lock-in thermography with modulated heating, contrary to the pulsed one, not only allows of finding out surface distribution of power of infrared radiation emitted by the surface of the material under examination and distribution of the associated temperature, but also enables us to determine distribution of amplitudes and

phases of thermal waves on the area in question. Amplitude of a thermal wave found on the basis of detected IR radiation emitted by the examined surface depends on the emissivity of the surface, whereas the phase is independent of this emissivity. These are properties deemed the most important advantage of the lock-in thermography with modulated heating. When the examined surface is not uniformly heated or the subsurface layer has been altered due to operating conditions, emissivity is locally affected. When the phase shifts have been mapped against the stimulating signal, one can infere the presence of flaws under the material surface (Oliferuk, 2008).

The pulsed phase thermography combines advantages of the pulsed thermograpy and the lock-in thermography with modulated heating. The response signal recorded with a thermovision camera represents the relationship between the surface temperature and time $T(t)$ for particular locations of the surface being cooled down after treating it with a thermal pulse. The signal is then subjected to discrete Fourier transformation (Oliferuk, 2008), which allows of finding particular waves for each point of the thermal image of the examined surface, and of development of phase maps. The phase maps, as in the method of the lock-in thermography with modulated heating, reveal locations of flaws in examined materials. The basic difference between the pulsed phase thermography and the lock-in thermography with modulated heating is that the pulsed phase thermography is focused on the analysis of a non-stationary process, i.e. the cooling of the surface of the object under examination, earlier treated with a thermal pulse. On the contrary, the lock-in thermography with modulated heating is applicable to stationary processes, i.e. stationary oscillations of the temperature field on the examined surface as a result of harmonic stimulation by heat (Oliferuk, 2008; Maldague, Matinetti, 1996; Maldague *et al*, 2002; Saenz *et al*, 2004).

5.3 Application of the thermographic method to assess condition of gas turbine vanes/blades

The pulsed thermography method was applied to a number of studies, including the project intended to determine the applicability of the method to assess flow capacity of internal cooling channels of turbine vanes/blades. Improvement in general efficiency of the turbine and increase in the power/weight ratio are directly associated with the exhaust-gas temperature. Increase in the exhaust gases temperature due to material problems has enforced application of turbine vanes/blades of more sophisticated geometrical shapes. It has, in turn, complicated vane/blade manufacturing processes and many other treatments, e.g. cooling the blades and vanes. Operational experience and examination of vanes and blades in repair workshops have demonstrated that, besides material defects, also disturbances in the internal cooling system caused by obstructions in cooling channels quite frequently cause defects of vanes and blades. Fig. 35 presents images of a damaged vane, taken with a conventional optical method, the raw pulsed thermography and the TSR (Thermographic Signal Reconstruction) technique employed in tomography devices. Application of the pulsed thermography method together with the dedicated software enables easy inspection of the internal system of cooling channels and flow capacity thereof. The advantages of the proposed method, as compared to the X-ray technique, are as follows: it keeps the operator safe from the hazardous X-ray radiation and, in consequence, does not require any dedicated, purposefully safeguarded rooms to carry out the examination; the unit cost of a test is reduced as there is no need to purchase expensive consumables; results are obtained in a very short time. The method based on the measurement of the amount of fluid flowing via the cooling channels within the blade offers much less accuracy and is more time- and labour-consuming than the thermographic technique.

Results of examining turbine vanes and blades with the pulsed thermography methods while investigating into discontinuities in the subsurface layer of the material became the inspiration to embark upon further research on the feasibility of this thermographic technique to assess alterations in microstructures of gas turbine blades and vanes using available devices and instruments. The examination involved specimens from new blades made of the EI 867-WD alloy and subjected to thermal ageing in a furnace at various temperatures. What resulted were distinct changes in the relationships between parameters of the thermal response from specimen materials and stimulation by a thermal pulse (Fig. 36).

Fig. 35. Images of high-pressure turbine blades (aircraft engine), acquired with various methods: optical, raw, TSR (Thermal Wave Imaging, Inc., 2009)

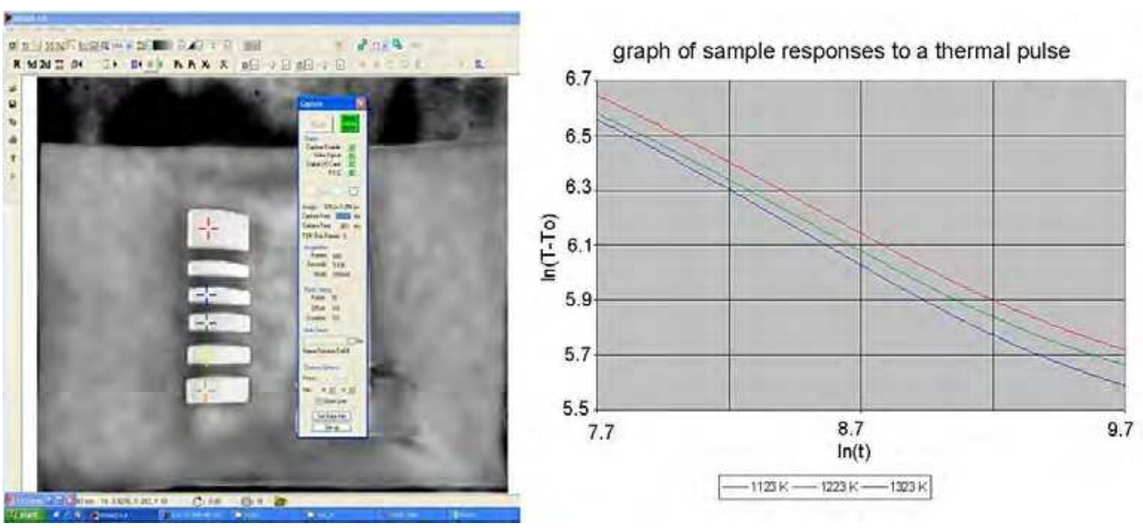

Fig. 36. Images of specimens cut out from blades (EI 867-WD alloy) subjected to soaking at 1123 K, 1223 K, 1323 K; graph of their responses to a thermal pulse

After completion of metallographic examination, the assessment of changes in micro-structures of the specimens was carried out, mainly of change in the strengthening γ′ phase -

$Ni_3(Al,Ti)$. Findings of this examination are presented in Fig. 37 as a nomogram. The relationship between the thermal response of the specimen's material, represented as the value of ln(T-To) against the average size of the γ′ precipitates allows of the assessment condition/health of the specimen material. This relationship, in conjunction with the knowledge on permissible changes in the microstructure, serves as a basis to judge whether the specimen's material remains fit for further service, or not.

High temperature results in both changes in thickness of the aluminium coating and modification of the γ′ phase structure. The examined microstructure of the subsurface layer reflects changes in the EI 867-WD alloy and proves the alloy structure suffered overheating as soon as the specimens were subjected to soaking at 1223 K (Figs 9 and 10). When the material criterion is adopted, i.e. a change in the size of γ′ precipitates, a threshold value of their remaining serviceable (fit for use) is considered the criterion that determines suitability of the blades for further operation. Results from metallographic examination confirm that the vane/blade material loses its high-temperature creep resistance at temperatures above 1223 K due to the clustering of fine-grain (Fig. 9) cubical particles of the γ′ phase and formation of plates (Fig. 10).

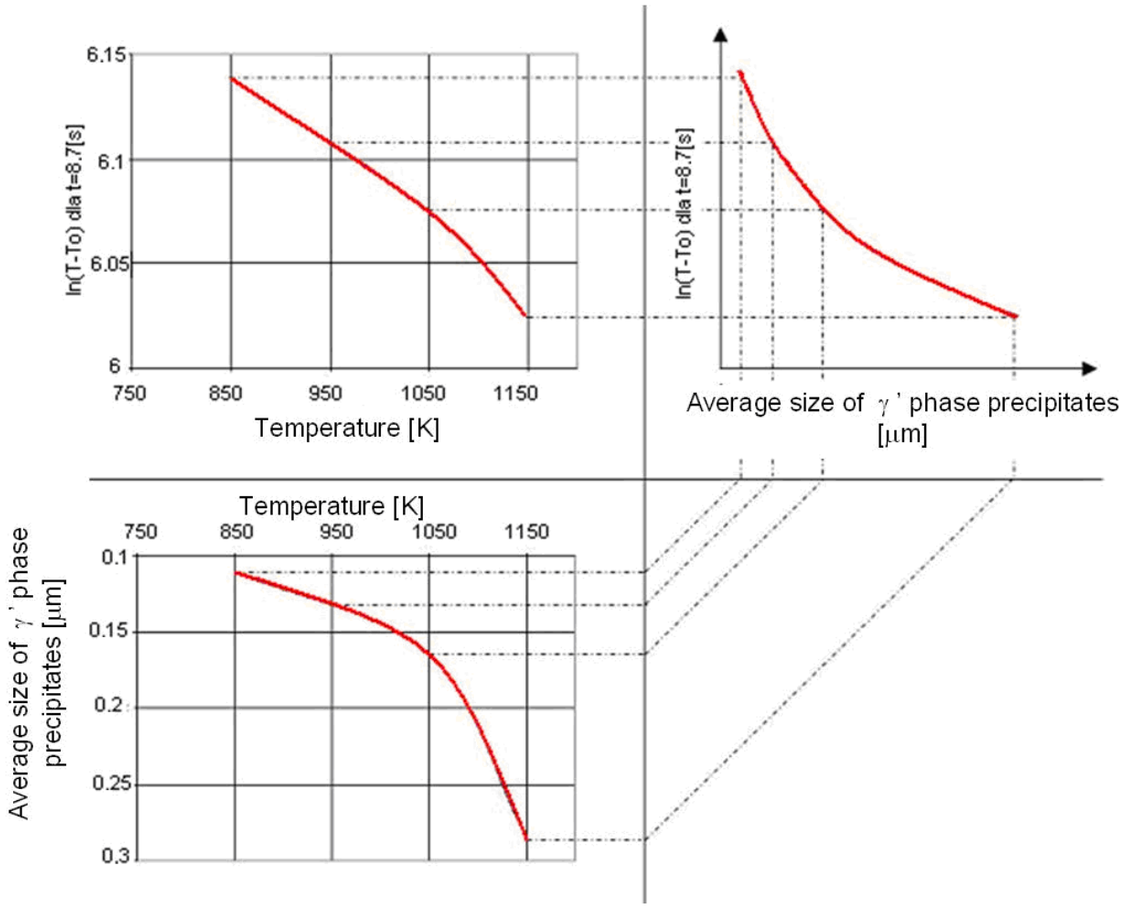

Fig. 37. Nomogram for the assessment of microstructures of specimens from gas turbine blades made of EI 867-WD alloy on the basis of relationship between change in *ln(T-To)* parameter and that in size of γ′ precipitates at different soaking temperatures

Further on, cognitive examination of items in service was carried out with the thermographic method. The examination was focused on the gas turbine stator vanes from the aircraft jet engine, the items in question being made of the ŻS6K alloy.
The vanes were initially classified according to the degree of overheating (from I to V) on the basis of visual criteria used in the course of engine inspection/overhaul. Results of the examination performed with the pulsed thermography have demonstrated that thermal response of the material of a vane deemed 'fit for service' (1st category) is rather uniform over the entire vane surface (Fig. 38). On the other hand, based on the analysis of response of a vane classified as 'unfit for service' to a thermal pulse one could easily find vane-surface areas that explicitly differed from the average. These areas overlapped the regions earlier classified, by visual inspection, as overheated. These findings, together with results of examining specimens cut out from vanes, serve as a basis to draw inferences on possible change in the material structure.
The already completed analyses of results obtained from the examination of vanes remaining in service and classified to the 1st and 5th category, and of new vanes, prove the pulsed thermography is suitable to judge about changes in the structure of material of turbine vanes remaining in service.

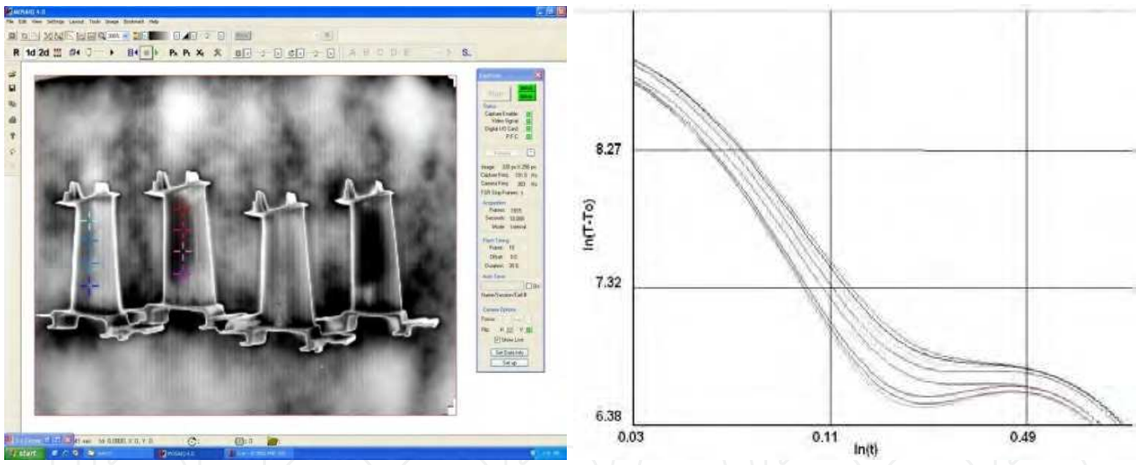

Fig. 38. Images of turbine vanes remaining in service , classified to the 1st and 5th categories (right); plotted are responses of vane materials to a thermal pulse

6. Conclusion

The assessment of health/condition of turbine blades and vanes is carried out by a diagnostic engineer on the basis of the recorded image of the component to be diagnosed, by comparing this image with pattern images of surfaces of turbine blades/vanes of the same type taken for items fit/unfit for use. However, such assessment criteria are very inaccurate since the diagnostic examination of blades/vanes is burdened with the element of subjective assessment (the organoleptic assessment of item condition). Moreover, colours depend on a number of physical and psychological factors. Therefore, the assessment

performed by a diagnostic engineer is associated with a significant risk of a human error. The destruction process in a gas turbine blade/vane begins with a failure to the protective aluminium coating (which is visible on the blade/vane image as a change in colour of the surface). Application of digital image-recording technology, together with the computer-aided analysis of images and the computer-aided decision-making process (neural networks), significantly contribute to the improvement in the diagnosis of that turbine component. Additionally, the use of an instrument capable of recording images of blade/vane surfaces (e.g. videoscopes) allows of the diagnosing with no need to have the turbine disassembled. Diagnostic information collected in that way is gained pretty fast and the cost of data acquisition is really low as compared to other inspection procedures.

This study presents fundamentals of the new method dedicated to the assessment of condition of gas turbine blades/vanes, applicable to both new vanes (the laboratory experiment) and already operated ones (actual operating conditions). The method involves the digital processing and analysis of surface images. Results obtained from the diagnostic examination of vanes already in service are confirmed by two methods developed to scan surface images, i.e. the scanning method based on colour profiles and one that involves the value of criteria plane. Both methods enable determination of the size (dimensions) of local areas of overheating (the percentage ratio of overheated surface area to the overall area of the vane) and thus, allow of the assessment of the overheating degree.

The application of artificial neural networks clearly demonstrates the feasibility of a fully automated (computer-aided) decision-making process, where parameters of images, earlier obtained from histograms and the co-occurrence matrix, are classified and sorted according to their applicability during the neural-network teaching process. Therefore, the application of an artificial neural network enabled clear and complete mapping of sophisticated relationships between images of a blade/vane surface and condition thereof. The presented results for the two-state classification (fit-for-use status – the non-overheated blade/vane and the unfit-for-use status – the overheated blade/vane) are highly promising. Moreover, the three-state classification is presented as well, with the diagnostic process enhanced by the possibility to approve the blade/vane for further, however supervised operation, i.e. until the date of scheduled periodic inspection and condition assessment.

However, for further thorough investigation into the impact of the working agent (the exhaust gas) on the condition of surfaces of blades/vanes, it is necessary to pay more attention to the effect the operating conditions have upon turbine blades/vanes: to 'isolate' the most damaging periods of the engine operation (the start-up and acceleration) since thermal shocks are the most destructive factors affecting each engine. They are caused by massive variations of the exhaust gas temperature, the components of the hot section of the engine are exposed to. Other characteristics of the engine operation should be also taken into account, including the rotational-speed increase during the start-up of the engine, values and fluctuations of the exhaust gas temperature upstream the turbine.

The presented results of thermographic examination of gas turbine blades and vanes, both new ones and those that already in operation, explicitly prove that the method is perfectly suitable for the diagnosticing of the vane condition. These results serve also as evidence that relationships between thermal loads applied during the turbine operation, changes in signals of thermal responses attributable to blade/vane material and the microstructure

status of the turbine items in question really exist. They also give grounds for developing the essentials of a non-destructive thermographic method to assess the degree of the gas-turbine blade's/vane's material overheating.

The method of pulsed thermography offers also a number of benefits as compared to other techniques of non-destructive investigation, including short time required for obtaining the results and low unit cost of of the examination. The proposed method is expected to enable comprehensive analysis of the entire population of vanes and blades from a specific batch when they are submitted for verification to the repair workshop, instead of hardly reliable method that consists in the inferring on the condition of the entire set of items in question on the basis of destructive examination of one or two randomly selected pieces.

7. References

Błachnio, J. & Bogdan, M. (2008). Diagnostic procedures for the assessment of condition of gas turbine vanes in operation. *Diagnostics*, No.1(45), 2008, pp. 91-96, ISSN 641-6414.

Błachnio, J. (2009). The effect of high temperature on the degradation of heat-resistant and high-temperature creep resistant alloys. *Solid State Phenomena*, Vol. 147-149, pp. 744 – 752, ISSN: 1662-9779.

Błachnio, J. & Bogdan, M. (2010). A non-destructive method to assess condition of gas turbine blades, based on the analysis of blade-surface images, *Russian Journal of Nondestructive Testing*, Vol.46, No.11, pp. 860-866, ISSN 1061- 8309.

Bogdan, M. & Błachnio, J. (2007). The assessment of gas-turbine blade condition as based on the analysis of light reflected from the blade surface. *Archives of Transport,* Vol.19, No.4, pp. 5-16, ISSN 0866-9546.

Bogdan, M. (2008). An attempt to evaluate the overheating of gas turbine blades. *Journal of Polish CIMAC*, Vol.3, No.1, pp. 25-32, ISBN 83-900666-2-9, ISSN 1231-3998.

Bogdan, M. (2008). Computer processing of some surface images of engineering objects affected by high temperature conditions. *Acta Mechanica et Automatica*, Vol.2, No.3, pp. 19-23, ISSN 1898-4088.

Bogdan, M. & Błachnio, J. (2009). The assessment of condition of gas-turbine nozzle guide vanes, with digital analysis of images of guide-vane surfaces applied. *Journal of Polish CIMAC*, Vol.4, No.3, pp. 23-30, ISBN 83-900666-2-9, ISSN 1231-3998.

Bogdan, M. (2009). Diagnostic Examination of Gas Turbine Blades/Vanes by Means of Digital Processing of Surface Images. PhD Thesis, Technical University of Białystok, Białystok, Poland, (in Polish).

Decker, R. F. & Mihalisin, J. R. (1969). Coherency strains in γ hardened nickel alloys. *Trans. ASM,* Vol. 62,No. 2, pp. 481 – 489.

Dudziński, A. (1987). *The X-ray Structural Analysis of the EI-929 Alloy Subjected to Long-time Soaking,* PhD Thesis. Military University of Technology, Warsaw, Poland, (in Polish).

Dżygadło, Z. (et al.). (1982). *Rotor systems of turbine engines.* Communication and Communications Publishing, Warsaw, Poland, ISBN 83-206-0217-3 (in Polish).

Haralick, R. M. & Shanmugam K. (1973). Textural Features for Image Classification. *IEEE Transactions on Systems*, Vol. Smc-3, No.6, (November 2007), pp. 610-621, ISSN 0018-9472.

Haralick, R. M. & Shapiro L. G. (1992). *Computer and robot Vision*, Addison-Wesley, ISBN 0201569434, Addison-Wesley Longman Publishing Co., Inc. Boston, MA. USA.

Hernas, A. (1999). *Creep resistance of steel and alloys. Part 1.* Publishing House of the Silesian University of Technology, Gliwice, Poland, ISBN 83-88000-16-0 (in Polish).

Kerrebrock, J. L. (1992). *Aircraft engines and gas turbines (2nd edition)*, Massachusetts Institute of Technology (MIT), The MIT Press, ISBN-10 0262111624, ISBN-13 978-026211162.

Korczewski, Z. (2008). *Archives of marine engines endoscopy*, Publishing House of the Polish Navy University, Gdynia, Poland (in Polish).

Lewitowicz, J. (2008). *Fundamentals of Aircraft Operation*. Publishing House of the Air Force Institute of Technology, vol 4, Warsaw, Poland (in Polish).

Luikov, A. V. (1969). *Analytical Heat Diffusion Theory*, Academic Press, New York, USA.

Maldague,.B & Xavier. P.V. (2001). *Theory and Practice of lnfrared Technology for Nondestructive Testin,* Wiley Interscience, ISBN 0-471-18190-0, USA.

Mikułowski, B. (1997). *Creep resistant and heat resistant alloys – superalloys,* Publishing House of the AGH University of Technology, Cracow, Poland (in Polish).

Oliferuk, W. (2008). *Infrared Thermography in Non-Destructive Tests of Materials and Equipment*, Gamma Office, ISBN 978-83-87848-61-3 Warsaw, Poland (in Polish).

Poznańska, A. (2000). *Lifetime of vanes made of the EI-867 alloy and operated in aircraft engines from the aspect of non-uniform deformations and structural alterations.* PhD Thesis. Technical University of Rzeszów, Poland (in Polish).

Rafałowski, M. (2004). *Integrated Image Analyzers for Lighting Technology based Measurements and Evaluation of Object Shapes.* Publishing House of the Technical University of Białystok, ISBN 0867-096X, Białystok, Poland (in Polish).

Sieniawski, J. (1995). *Criteria and methods for the assesment of materials for components of turbine engines*. Publishing House of the Technical University of Rzeszów, Poland (in Polish).

Sims, C. T.; Stoloff N.S & Hagel, W. C. (1987). *Superalloys II. High temperature materials for aerospace and industrial power,* Wiley & Sons, New York, USA.

Sunden, B. & Xie, G. (2010). Gas Turbine blade tip heat transfer and cooling: A Literature Survey. *Heat Transfer Engineering,* Vol. 31, Issue 7, Taylor & Francis, pp. 527-554, ISSN 1521-0537 (electronic), ISSN 0145-7632 (paper).

Thermal Wave Imaging, Inc.(2009). "EchoTherm User Manual".

Tracton, A. A. (Ed.). (2006). *Coatings Technology: Fundamentals, Testing, and Processing Techniques*, CRC Press, ISBN 978-1-4200-4406-5, Bridgewater, New Jersey, USA.

Tracton, A. A. (Ed.). (2007). *Coatings Materials and Surface Coatings*, ISBN 978-1420-04404-1, CRC Press, Bridgewater, New Jersey, USA.

Zhang, D.; Kamel, M. & Baciu, G. (2004). *Integrated Image and Graphics Technologies*, Kluwer Academic Publishers, ISBN 1-4020-7774-2, Norwell Massachusetts,

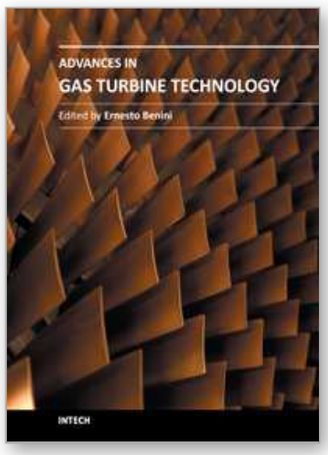

Advances in Gas Turbine Technology

Edited by Dr. Ernesto Benini

ISBN 978-953-307-611-9
Hard cover, 526 pages
Publisher InTech
Published online 04, November, 2011
Published in print edition November, 2011

Gas turbine engines will still represent a key technology in the next 20-year energy scenarios, either in stand-alone applications or in combination with other power generation equipment. This book intends in fact to provide an updated picture as well as a perspective vision of some of the major improvements that characterize the gas turbine technology in different applications, from marine and aircraft propulsion to industrial and stationary power generation. Therefore, the target audience for it involves design, analyst, materials and maintenance engineers. Also manufacturers, researchers and scientists will benefit from the timely and accurate information provided in this volume. The book is organized into five main sections including 21 chapters overall: (I) Aero and Marine Gas Turbines, (II) Gas Turbine Systems, (III) Heat Transfer, (IV) Combustion and (V) Materials and Fabrication.

INTECH
open science | open minds

InTech Europe
University Campus STeP Ri
Slavka Krautzeka 83/A
51000 Rijeka, Croatia
Phone: +385 (51) 770 447
Fax: +385 (51) 686 166
www.intechopen.com

InTech China
Unit 405, Office Block, Hotel Equatorial Shanghai
No.65, Yan An Road (West), Shanghai, 200040, China
中国上海市延安西路65号上海国际贵都大饭店办公楼405单元
Phone: +86-21-62489820
Fax: +86-21-62489821

IntechOpen